

NTD Ge sensor development for superconducting bolometers

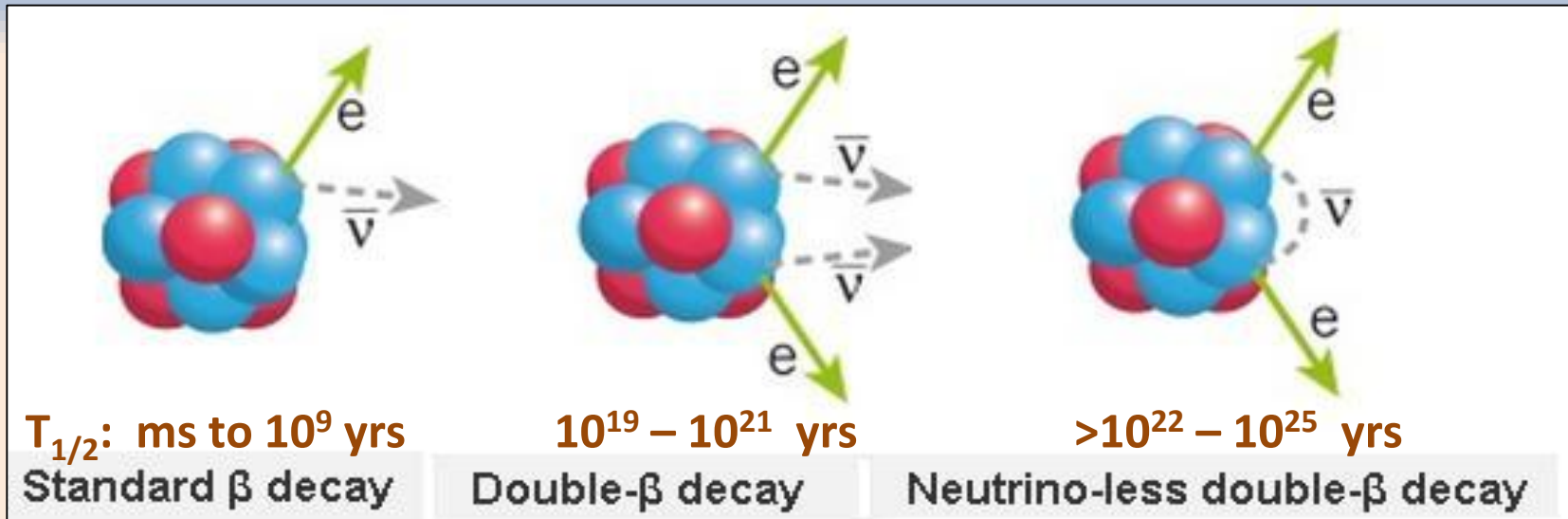
(for Neutrinoless Double Beta Decay)

S. Mathimalar
INO(TIFR) – HBNI
14/12/2015

Plan of the talk

- ❖ Sensor for cryogenic bolometer - Neutrino less Double Beta Decay (NDBD) experiment
- ❖ Neutron Transmutation Doping of Ge
 - Neutron Irradiation
 - Radioactive impurity studies
 - Defect studies in NTD Ge
 - Positron Annihilation Lifetime Spectroscopy (PALS)
 - Channeling
- ❖ Characterizing NTD Ge sensors
 - Fabrication of NTD Ge sensors
 - Hall Effect measurement
 - Low Temperature Measurement
- ❖ Summary

Neutrinoless Double Beta Decay (in ^{124}Sn)

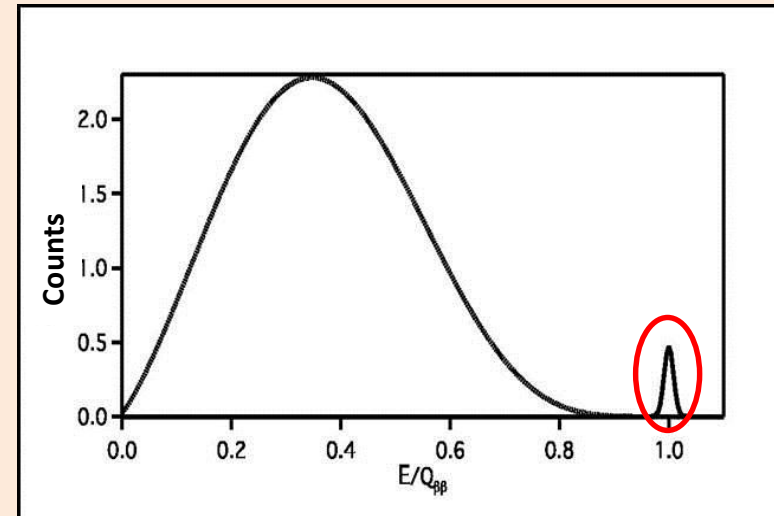


Significance of $0\nu\beta\beta$:

Presently the only experiment which can tell whether neutrino is its own antiparticle (Majorana particle) or not (Dirac particle)

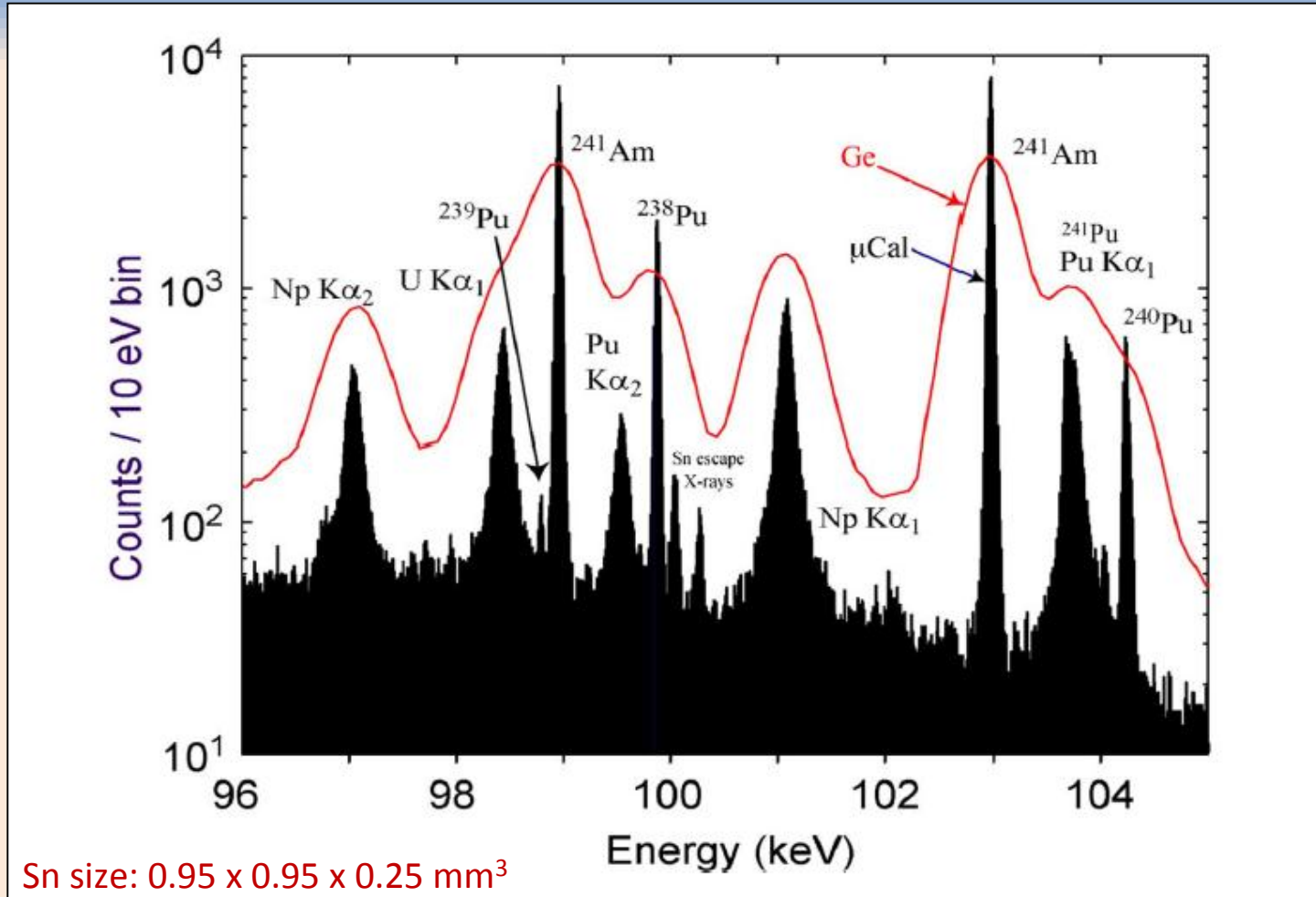
Experiments will look at:

Constancy of sum energy of two simultaneously emitted electrons, which requires high energy resolution and large scale detector



Experimental signature

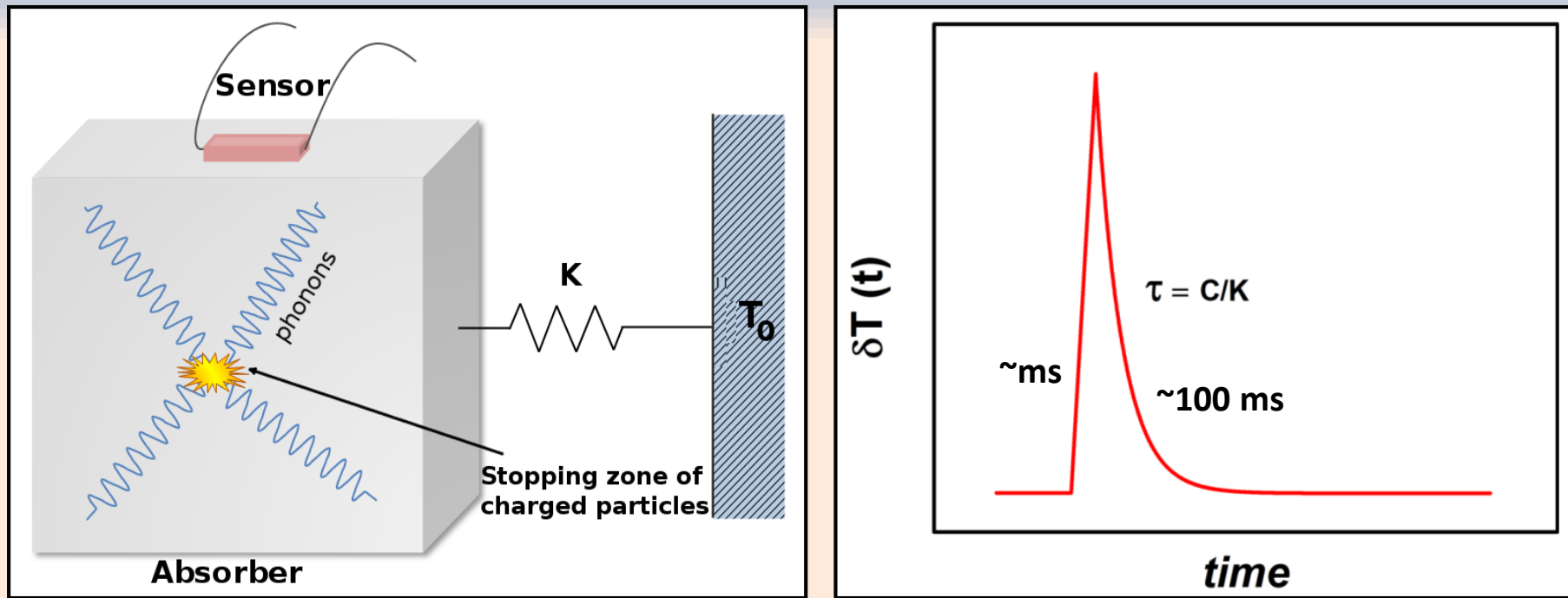
Sn micro-calorimeter



- ❖ Sn microcalorimeter @ 65 mK: 22eV FWHM @ 97.43keV
- ❖ Typical HPGe resolution 500eV

Figure from M.K. Bacrania et al., IEEE TRANSACTIONS ON NUCLEAR SCIENCE, 56 (2009) 2299.

Bolometer for NDBD



- ❖ When DBD occur, energy of electrons heats the crystal
- ❖ Thermalization leads to rise in the crystal temperature $T + \delta T$
- ❖ The detector will be operated at an optimum temperature of $\sim 10\text{mK}$, in order to get a reasonable δT ($\sim 100\mu\text{K}/\text{MeV}$).
- ❖ Need to reduce the addenda from all materials.
- ❖ Need a high sensitivity, reproducibility sensor works at mK.

Sensors used at mK

- ❖ Semiconductor thermistor (NTD Ge)
(semiconductor resistance dependence of the temperature)
- ❖ Transition edge sensors (TES)
(Superconducting transition resistance dependence of the temperature)
- ❖ Magnetic micro calorimeters (MMC) paramagnetic
(Magnetization dependence of the temperature)
- ❖ Multiplexed Kinetic Inductance Detectors (MKID)
(Temperature dependence of AC Impedance of a superconductor)

Bolometer sensors at mK

Essential properties :

- ❖ Low specific heat
- ❖ Fast rise time
- ❖ Radio pure
- ❖ Bare sensor (no packing material)
- ❖ High temperature sensitivity
- ❖ Mass producible
- ❖ Reproducibility

Commercially available :

- ❖ Carbon speer (resistance)
- ❖ RuO₂ (resistance)
- ❖ CMN (susceptibility)
- ❖ Melt growth doped semiconductor (resistance)
- ❖ Cerenox (resistance)

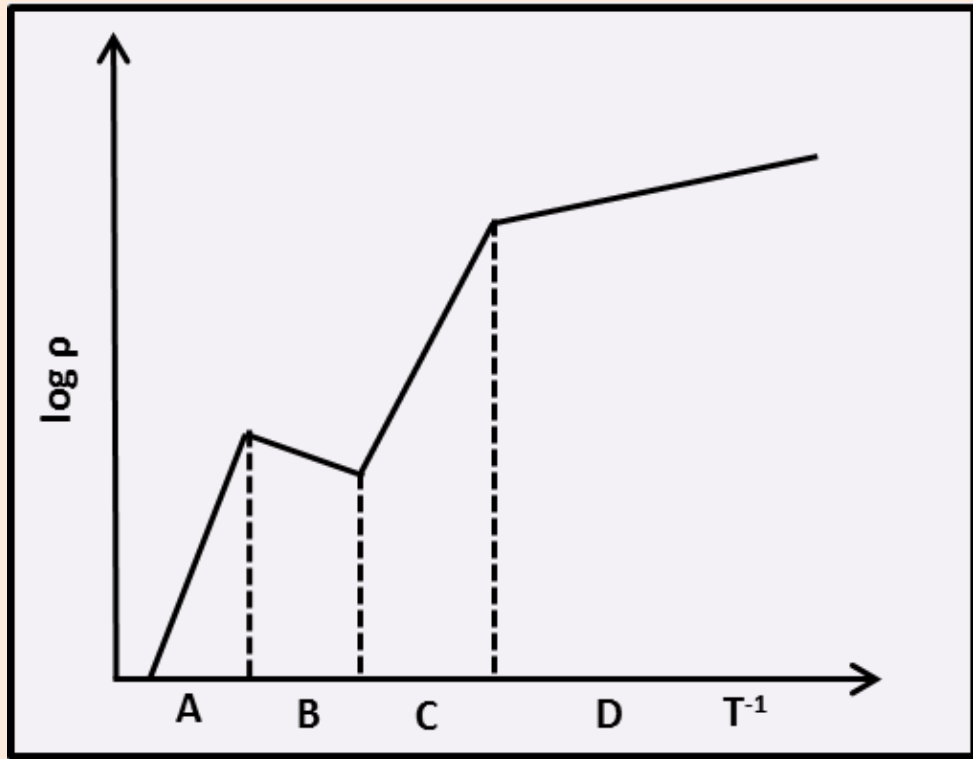
Preferable sensor:

- ❖ Most of the commercial sensors do not posses all the essential properties of a bolometric sensor.
- ❖ Hence sensors need to be developed indigenously for NDBD.
- ❖ Lightly doped semiconductor Ge posses most of the needed properties and it works on **Variable Hopping Mechanism (VRH)** at low temperature.
- ❖ The probability (P_{ij}) of carrier tunneling is given by,

$$P_{ij} = \begin{cases} \exp\left(-2\alpha R_{ij} - \frac{(E_j - E_i)}{K_B T}\right) & \text{if } E_j > E_i \\ \exp(-2\alpha R_{ij}) & \text{if } E_j \leq E_i \end{cases}$$

where R_{ij} – range; α - depends on potential height.

Temperature dependence of resistivity in a lightly doped semiconductor



Schematic temperature dependence of the resistivity of a lightly doped semiconductor

(A) Intrinsic conduction range
(B) Saturation range of impurity conduction

(C) Freeze-out range
(D) Hopping conduction range

For a Ge with $N_D \sim 10^{15}/\text{cm}^3$

A: $T > 400\text{K}$; B: $50 < T < 400\text{ K}$;
C: $7 < T < 50\text{ K}$; D: $T \sim 7\text{ K}$

Doping level should provide the sensor a measurable R as well as high dR/dT .

Figure from B.I. Shklovskii, A.L. Efros, *Electronic Properties of Doped Semiconductors*, Springer Publication (1984).

Neutron Transmutation Doped Germanium (NTD Ge) Sensor

- ❖ Neutron Transmutation Doped (NTD) Ge sensor is preferred due to its high temperature sensitivity, reproducibility, mass production, low specific heat, fast rise time and simple read out.
- ❖ Low neutron capture cross-section - homogenous doping. Melt-doped Ge with large concentration will be inhomogeneous and can have different characteristics

$$\rho = \rho_o \exp \left(\frac{T_o}{T} \right)^\alpha$$

- ❖ In a Variable Hopping mechanism, the α is predicted to be 0.5.
- ❖ ρ_o and T_o can be tuned by neutron fluence.

Dopant details of irradiated Ge

| Isotope | Isotopic Abundance (%) (SIMS) | | Products formed (half-life) | Decay into(decay mode) | Type |
|------------------|-------------------------------|-------|--------------------------------------|---|------|
| | Set 1 | Set 2 | | | |
| ⁷⁰ Ge | 21.5 | 21.9 | ⁷¹ Ge* (11.43 d) | ⁷¹ Ga (e ⁻ capture) | p |
| ⁷² Ge | 26.8 | 27.0 | ⁷³ Ge (stable) | ⁷³ Ge | - |
| ⁷³ Ge | 10.8 | 8.8 | ⁷⁴ Ge (stable) | ⁷⁴ Ge | - |
| ⁷⁴ Ge | 34.1 | 35.1 | ⁷⁵ Ge* (82.78min) | ⁷⁵ As (β-decay) | n |
| ⁷⁶ Ge | 6.8 | 7.2 | ⁷⁷ Ge* (11.3, 38.8hrs) | ⁷⁷ As*, ⁷⁷ Se (β, β-decay) | n |

❖ The net carrier concentration is given by

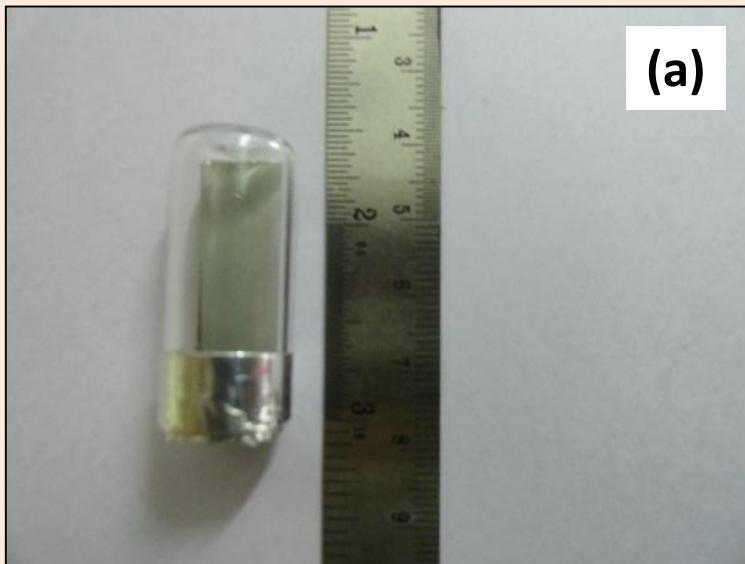
$$N_A - N_D = [N_{71Ga} - (N_{75As} + 2 \times N_{77Se})]$$

❖ For a natural Ge, the neutron doping results in **p-type** due to its isotopic abundance and thermal neutron capture cross section.

Neutron Transmutation Doping of Ge

Neutron Irradiation of Ge

- ❖ Semiconductor grade Ge irradiated with thermal neutron from Dhruva Reactor (max. power 100MW), Bhabha Atomic Research Centre (BARC).
- ❖ Samples were cleaned, wrapped with (a) quartz tube or (b) High purity Aluminium foil, cold sealed in Al container, placed in the permissible region of reactor and then irradiated with reactor neutrons.
- ❖ Packing material has been carefully chosen to minimize the residual radioactive contamination.

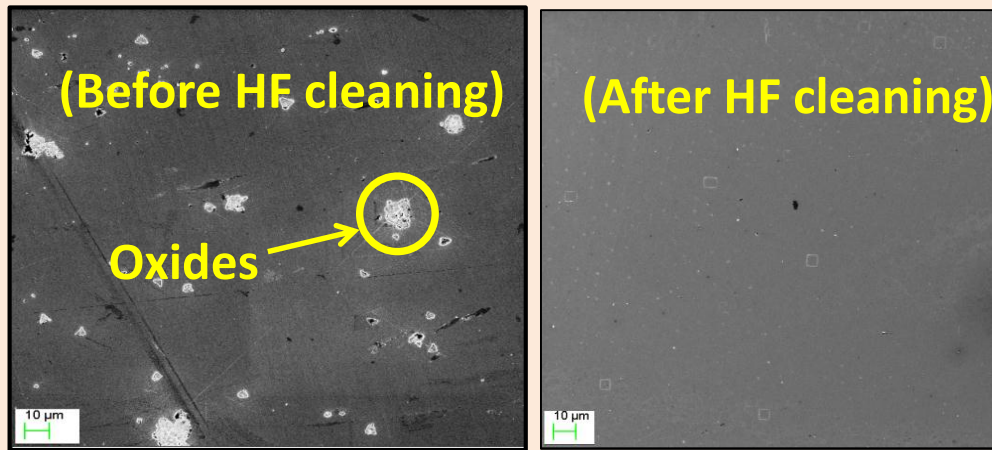


Samples details with neutron fluence

| Samples (Plane, Thickness, Resistivity) | Tag (size in mm ²) | Neutron fluence (n/cm ²) | | |
|--|--------------------------------------|--------------------------------------|---------------------------------------|------------------------------|
| | | Thermal (<0.625eV) | Epithermal (.625eV - 0.821 MeV) | Fast (.821MeV - 10MeV) |
| Set 1 (<111>, 0.4 mm, >30 Ωcm) | B (10 x 10) | 1.40×10^{19} | 2.56×10^{18} | 1.72×10^{17} |
| | C (10 x 10) | 9.13×10^{18} | 1.72×10^{18} | 1.12×10^{17} |
| Set 2 (<100>, 1.0 mm, >35 Ωcm) | D (30 x 10) | 4.57×10^{18} | 8.02×10^{17} | 5.32×10^{16} |
| | E (30 x 10) | 2.11×10^{18} | 3.52×10^{17} | 2.46×10^{16} |
| | F (30 x 10) | 3.52×10^{18} | 5.87×10^{17} | 4.11×10^{16} |
| | G (30 x 10) | 3.57×10^{18} | 5.95×10^{17} | 4.16×10^{16} |
| | H (10 x 10) | 1.8×10^{18} | 3.01×10^{17} | 2.1×10^{16} |
| | I (30 x 10) | 1.8×10^{18} | 3.01×10^{17} | 2.1×10^{16} |

Surface studies and annealing details

- ❖ Samples were cleaned with HF for 90sec and rinsed with distilled water and then blow dried with dry N₂ at every stage of measurement.
- ❖ SEM images before and after etching shows removal of oxide layer from Ge surface with HF treatment.



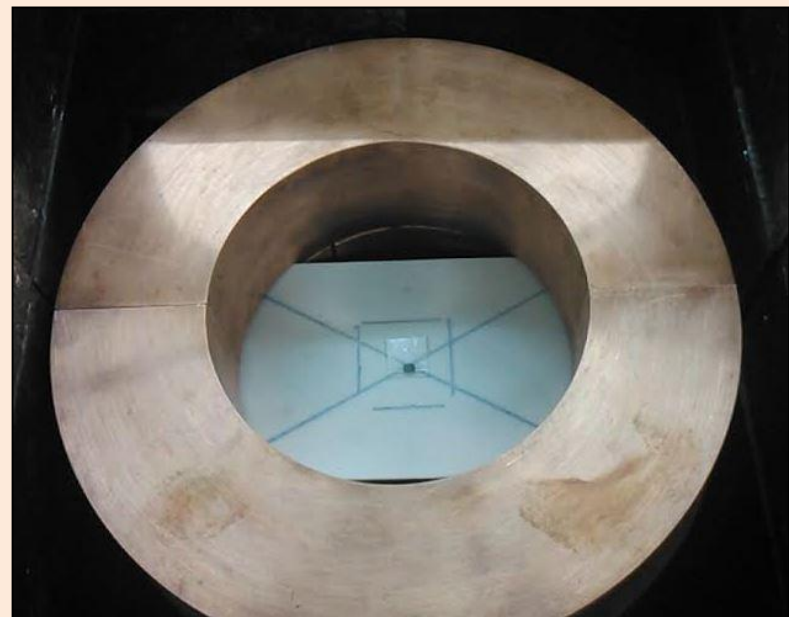
- ❖ The samples were annealed at 600°C for 2 hours in a sealed quartz tube to cure defects and were cut into the required size for various studies.

Radioactive Impurity Studies



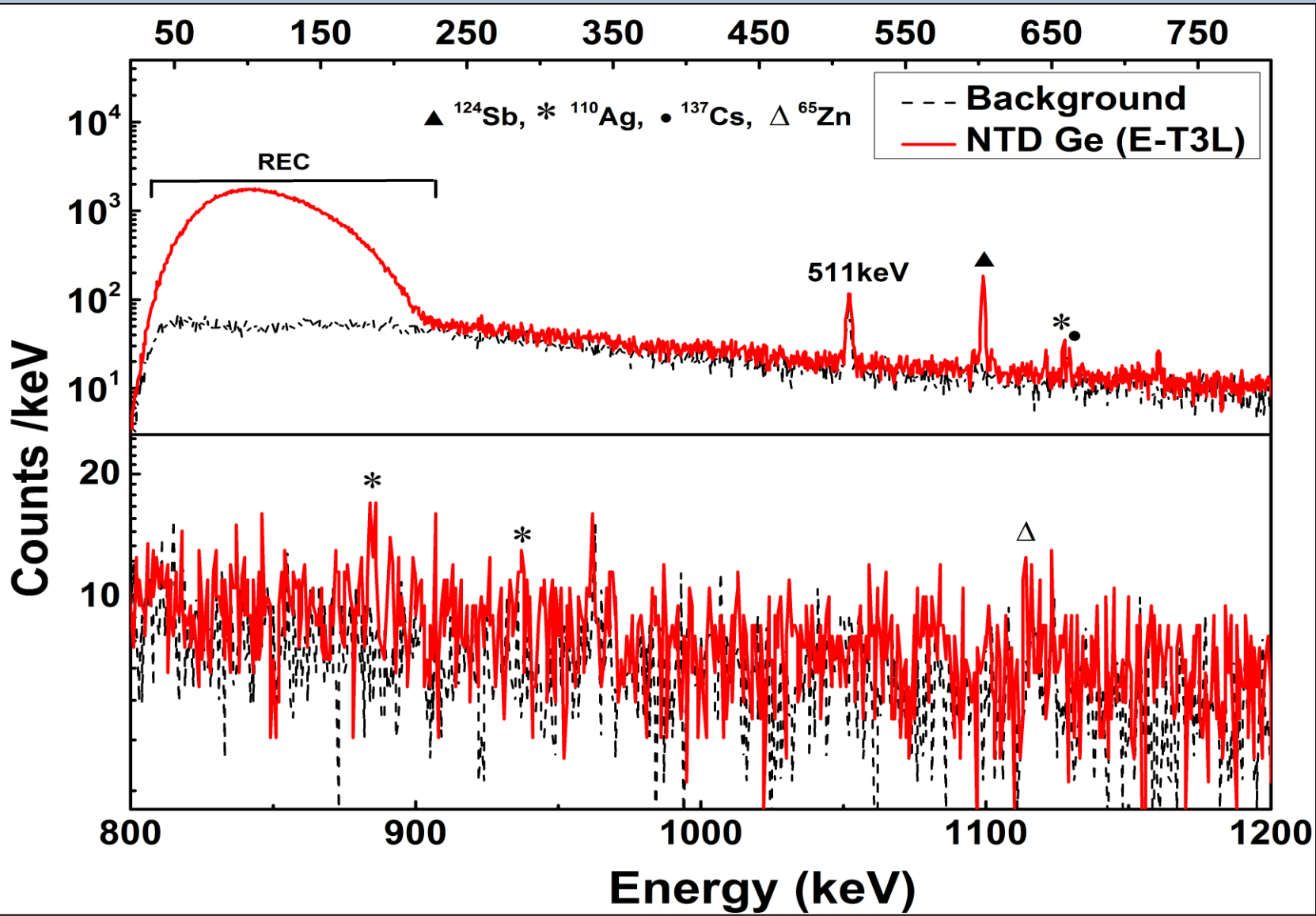
N. Dokania et al., NIM A, 745, (2014) 119

Sample mounted on HPGe detector
(top view)



- ❖ Irradiated NTD Ge wafers were studied for the radioactive contaminants using low background HPGe detector.
- ❖ The detector was shielded with Cu and low activity Pb to reduce the room background.

Radioactive Impurity studies (contd...)

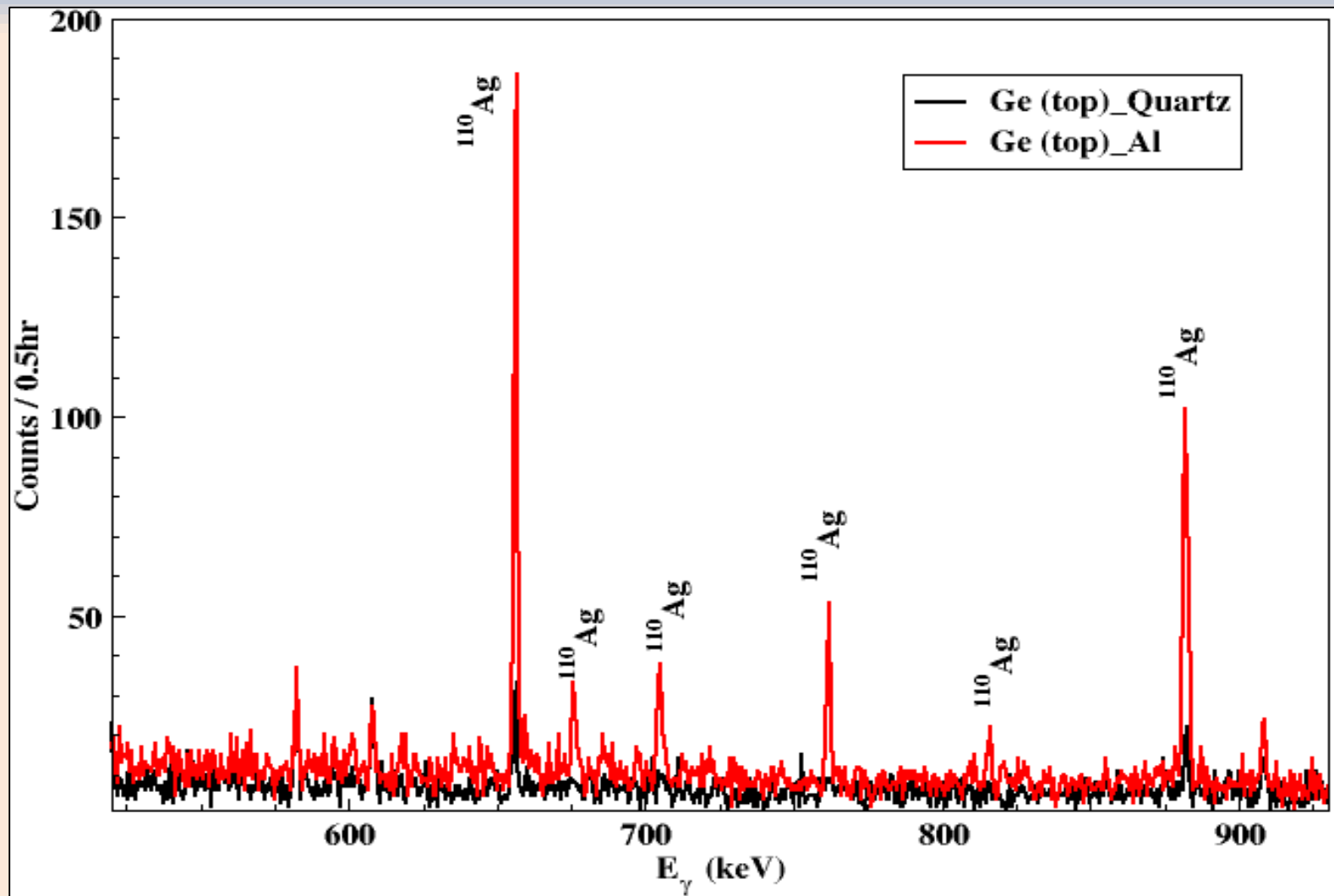


Observed impurities in the Un-etched NTD Ge sample

| Radionuclide | Half-life | E _γ (keV) | Relative Intensity (%) |
|--------------------|-----------|-------------------------|---------------------------|
| ⁴⁶ Sc | 83.79 d | 889.3 | 99.98 |
| | | 1120.5 | 99.99 |
| ⁵¹ Cr | 27.7 d | 320.1 | 9.91 |
| | | 1099.3 | 56.5 |
| ⁵⁹ Fe | 44.5 d | 1291.6 | 43.2 |
| | | 1173.2 | 99.85 |
| ⁶⁰ Co | 5.27 y | 1332.5 | 99.98 |
| | | 1115.5 | 50.04 |
| ⁶⁵ Zn | 243.66 d | 657.8 | 95.61 |
| | | 884.7 | 75.0 |
| ^{110m} Ag | 249.76 d | 937.5 | 35.0 |
| | | 602.7 | 97.8 |
| ¹²⁴ Sb | 60.2 d | 1691.0 | 47.57 |
| | | 722.8 | 10.76 |
| ¹⁸² Ta | 114.74 d | 1121.3 | 35.24 |
| | | 1221.4 | 27.23 |
| | | 1231.0 | 11.62 |

- ❖ Trace radioactivity in sensors can produce significant background for rare event studies
- ❖ The radioactive contaminants can also act as a heat load when the sensors are used in mK temperature
- ❖ Radioactive impurities with longer half life are of more concern.

Comparison of Quartz and Al wrapped NTD Ge samples

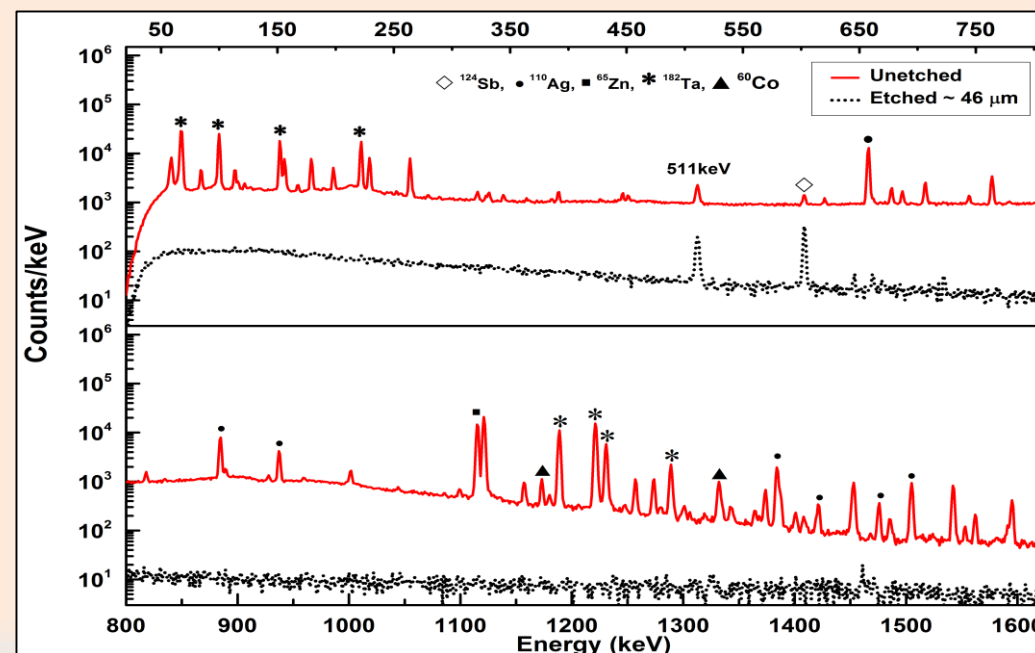


Al wrapped samples shows higher activity compared to samples placed in quartz

Radioactive Impurity studies (contd..)

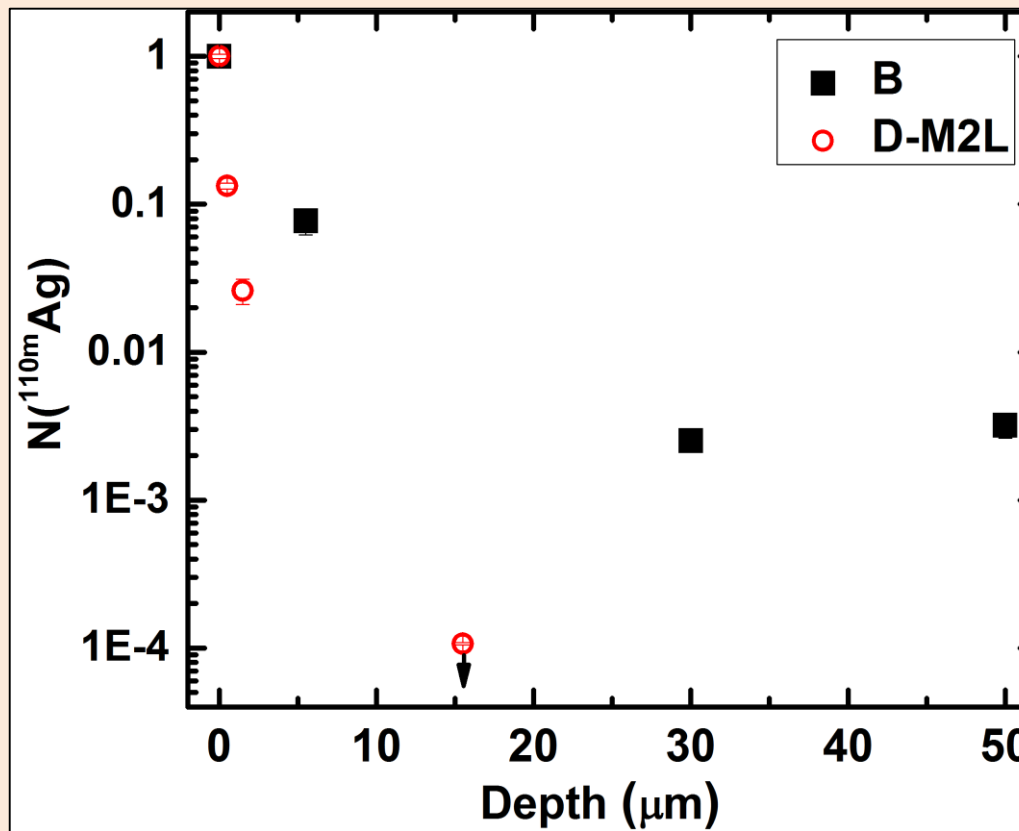
Sources of Radioactive impurities:

- ❖ Neutron induced reaction products of impurities in bulk Ge
- ❖ Neutron induced reaction products of residual impurities in the Ge surface(resulting from contamination during lapping/polishing/cutting)
- ❖ Neutron induced reaction products from wrapping material which can get recoil implanted in Ge
- ❖ Deposition and thermal diffusion of radioactive contaminants from the surrounding environment in the sample capsule resulting from long exposures at high temperatures during irradiation (80°C).
- ❖ The samples were etched step wise with H_2O_2 at 80°C in sonicating bath.
- ❖ Spectra of etched and unetched sample D-B1 ($\Phi_{\text{th}} = 4.6 \times 10^{18}/\text{cm}^2$).
- ❖ Reduction in radioactive contaminant is visible after etching.



Depth profile of radio-impurities

- ❖ Set 1 and Set 2 samples showed different impurities.
- ❖ Set 1 samples showed ^{110}Ag , whereas Set 2 showed ^{124}Sb activity even after etching $\sim 50 \mu\text{m}$ etching.

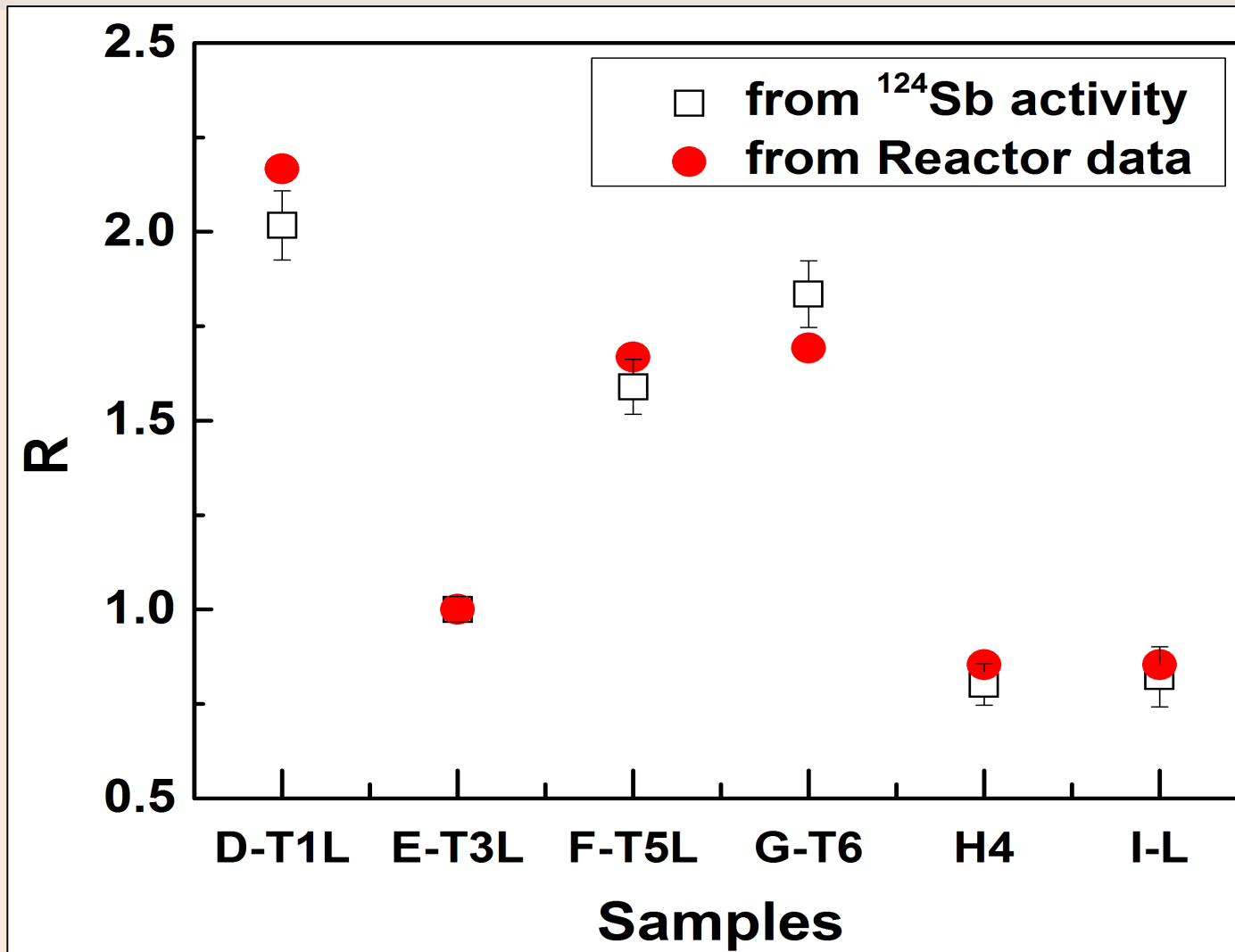


Radioactive profile of ^{110}Ag in $<111>$ (B) and $<100>$ (D-M2L) set samples

Observed radioactive impurities as a function of the etched depth (d) in different samples.

| Sample | observed radio-nuclides | | |
|--------|--|---|---------------------------|
| | d = 0 μm | d = 10–20 μm | d = 50–60 μm |
| B | ^{60}Co , ^{65}Zn , $^{110\text{m}}\text{Ag}$, ^{182}Ta | - | $^{110\text{m}}\text{Ag}$ |
| C | ^{60}Co , ^{65}Zn , $^{110\text{m}}\text{Ag}$, ^{182}Ta | - | $^{110\text{m}}\text{Ag}$ |
| D-T1 | ^{60}Co , ^{65}Zn , $^{110\text{m}}\text{Ag}$, ^{124}Sb , ^{182}Ta | ^{60}Co , $^{110\text{m}}\text{Ag}$, ^{124}Sb | ^{124}Sb |
| D-M2L | ^{60}Co , ^{65}Zn , $^{110\text{m}}\text{Ag}$, ^{124}Sb , ^{182}Ta | ^{124}Sb | - |
| D-B1 | ^{60}Co , ^{65}Zn , $^{110\text{m}}\text{Ag}$, ^{124}Sb , ^{182}Ta | ^{124}Sb , $^{110\text{m}}\text{Ag}$ | ^{124}Sb |
| E-T3L | ^{124}Sb , $^{110\text{m}}\text{Ag}$ | ^{124}Sb , ^{65}Zn | ^{124}Sb |
| F-B5 | ^{124}Sb , $^{110\text{m}}\text{Ag}$, ^{65}Zn | ^{124}Sb | ^{124}Sb |

^{124}Sb activity proportional to neutron fluence



The relative neutron fluence (R) scales with the activity of ^{124}Sb

Radioactive Impurity estimation

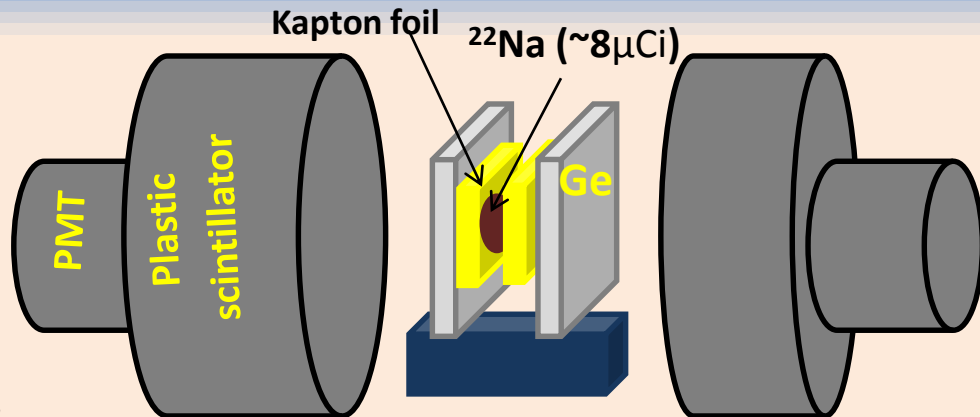
| Samples | Activity (mBq/gm) ($t_0 + 150$ days) | | T_{cool} (yrs) | ^{123}Sb Conc. (ppt) |
|---------|---------------------------------------|-------------------|---------------------|----------------------------------|
| | ^{110}Ag | ^{124}Sb | | |
| B | 3018 ± 465 | < 26.6 | 9 | - |
| C | 743 ± 222 | < 18.6 | 7 | - |
| D-B1 | < 2.0 | 420 ± 9 | 1.9 | 115 (2) |
| E-T3L | < 2.5* | 201 ± 20 | 1.7 | 119 (12) |
| F-B5 | < 2.9 | 344 ± 12 | 1.8 | 123 (4) |

* Estimated from E-T3L sample

The concentration of ^{123}Sb is ~ 120 ppt in Set 2 and about 2 years of cool down period is required for the activity to reduce $<1\text{mBq/gm}$ and to use the samples as sensors in rare decay process.

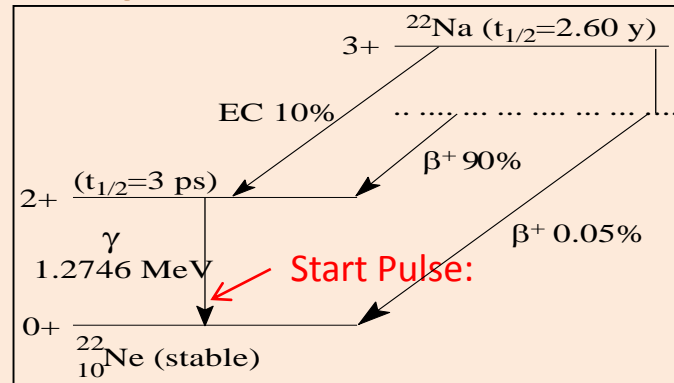
Defect studies – Positron Annihilation Lifetime Spectroscopy (PALS)

- ❖ PALS probe defects via **positron lifetime measurement**
- ❖ Positron interacts with Ge sample, experiences: attractive (due to e^- s) and repulsive force (due to core ions)
- ❖ Defect free crystal, positron interacts with the valance electron results in two γ rays of 511 keV due to annihilation.
- ❖ Positron interacts in a crystal with defects, more likely get trap in the defects due to repulsive force of ions. Results in longer positron lifetime.
- ❖ Larger the defect, longer the lifetime of the positron.



❖ **Counts:** $\sim 3 \times 10^6$ events; **Count rate:** ~ 50 cps

Decay scheme of a ^{22}Na nucleus



Stop Pulse: 511keV (γ -ray resulting from annihilation in the crystal)

PALS Results

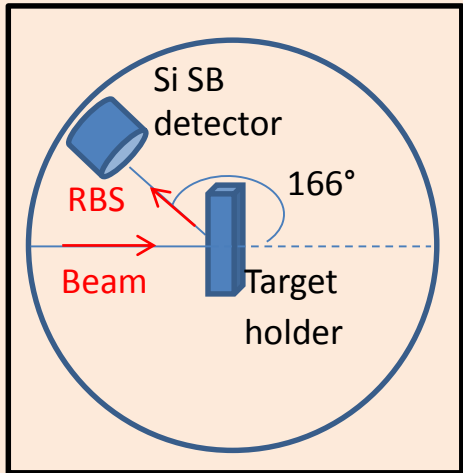
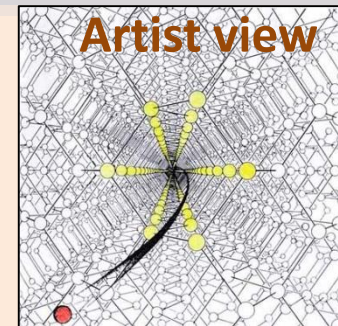
| Plane | Samples | Φ_{th} (n/cm ²) | T _{$\beta+$} (ps) | †Ref (ps) |
|------------------|--------------|----------------------------------|---------------------------------------|------------|
| <111> (Set 1) | Virgin Ge | - | 227.8 ± 0.3 | 228 (Bulk) |
| | Irradiated B | 1.40×10^{19} | 293.6 ± 0.4 | 293* |
| | Annealed B | | 225.6 ± 0.3 | 228 (Bulk) |
| <100> (Set 2) | Virgin Ge | - | 232 ± 0.3 | 228 (Bulk) |
| | Irradiated D | 4.57×10^{18} | 294 ± 0.3 | 293* |
| | | | 401 ± 30 | 401 |
| | Annealed D | | 233 ± 0.4 | 228 (Bulk) |
| | Irradiated E | 2.11×10^{18} | 293.5 ± 0.4 | 293* |
| | Annealed E | | 228 ± 0.4 | 228 (Bulk) |
| | Irradiated F | 3.52×10^{18} | 294 ± 0.6 | 293* |

- ❖ Most of the irradiated samples showed defects of Monovacant, except higher dose in Set 2, which had vacancy cluster as well.
- ❖ All the annealed samples has positron lifetime close to that of the un-irradiated (bulk) sample.

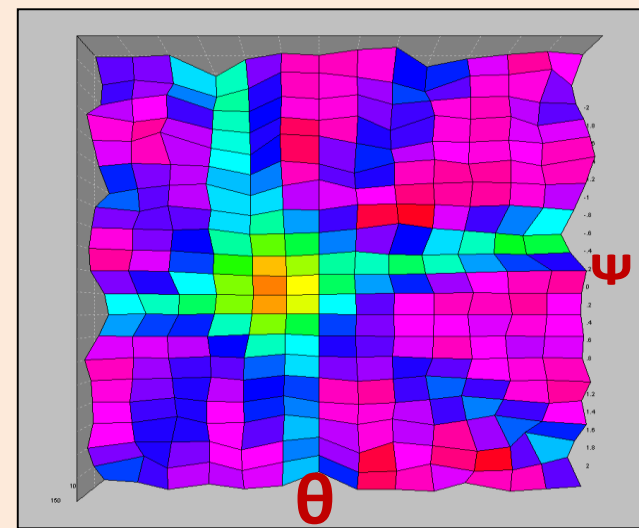
†Ref: R.K. Rehberg, H.S. Leipner, *Positron Annihilation in Semiconductors - Defect Studies*, Springer Publication (1999)

Channeling studies

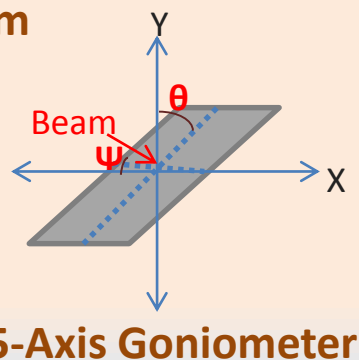
- ❖ NTD Ge crystal probed with an energetic alpha beam ($\sim 2\text{MeV}$) along the axial direction at **PARAS facility, IUAC, New Delhi**.
- ❖ Defects lead to dechanneling of the beam, results in higher Rutherford Back Scattering (RBS) yield
- ❖ Minimum current – avoids damage produced during measurement.



Schematic diagram

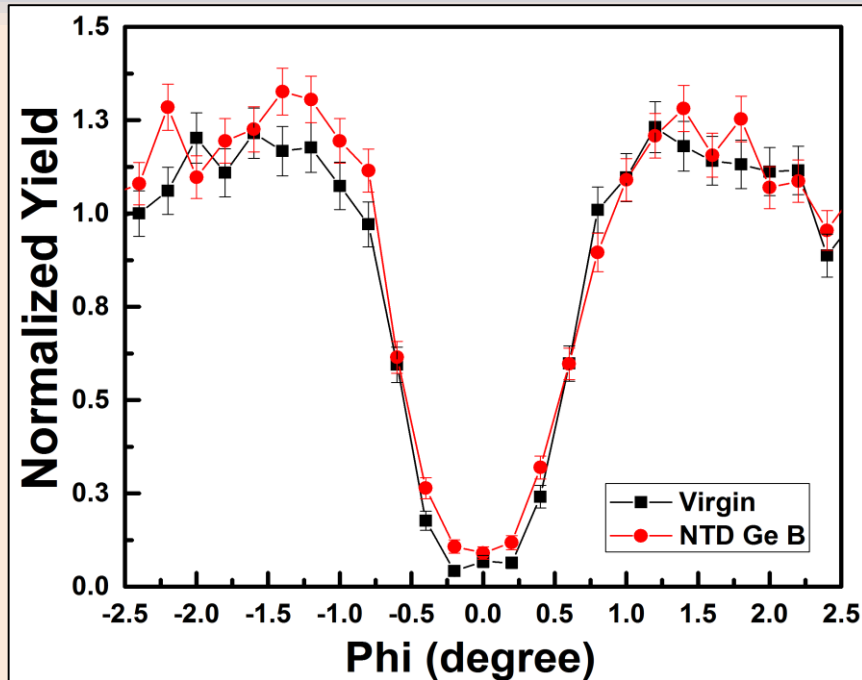


2D Image of Ge crystal $<100>$ cleavage plane

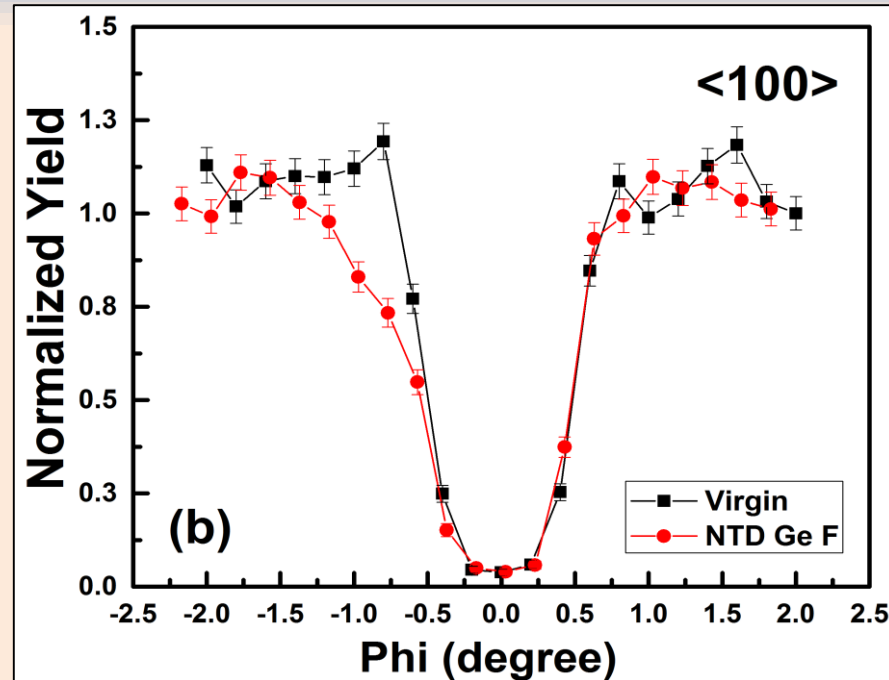


5-Axis Goniometer

Axial dip of the NTD Ge



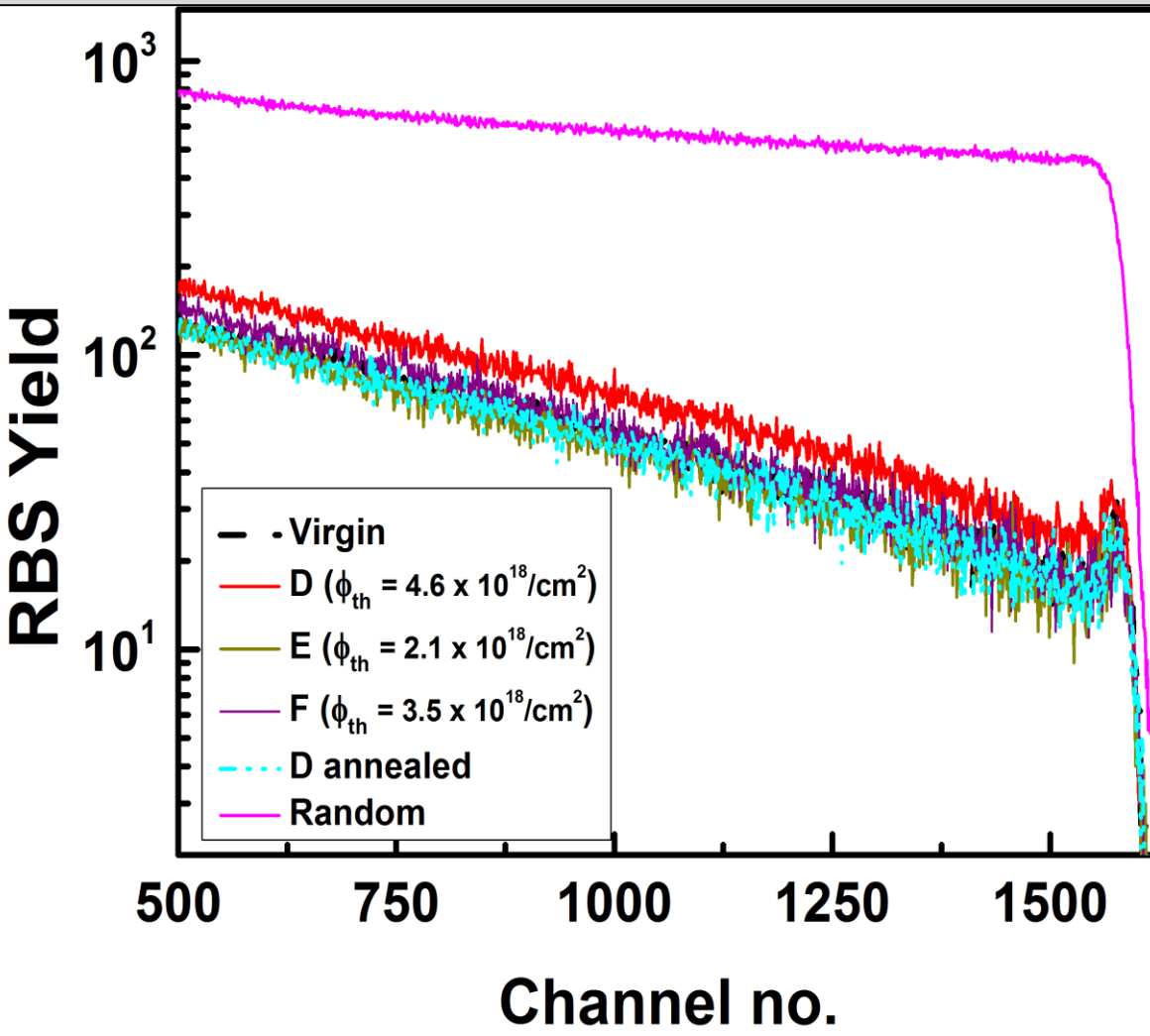
Axial dip of NTD Ge <111> sample



Axial dip of NTD Ge <100> sample

- ❖ Axial dip of both <111> and <100> did not showed a significant change.
- ❖ Left side of axial dip of <100> NTD Ge F shows the planar effect.

Channeled spectra and random spectrum of <100>



- ❖ Higher neutron dose samples showed change in the RBS yield, whereas the lower dose no difference in the RBS yield
- ❖ The irradiated sample D – higher RBS yield
- ❖ Annealed sample D – close to virgin sample.
- ❖ Indicates annealing recovered the defects in the irradiated crystal.

Defect density estimation

Defect density calculated to a depth of 316nm (100keV) just below the surface.

The defect density is calculated using relation

$$N_D = N \left(\frac{\chi_{min}^{irr} - \chi_{min}^0}{1 - \chi_{min}^0} \right)$$

Where χ_{min} = channelled RBS/random RBS

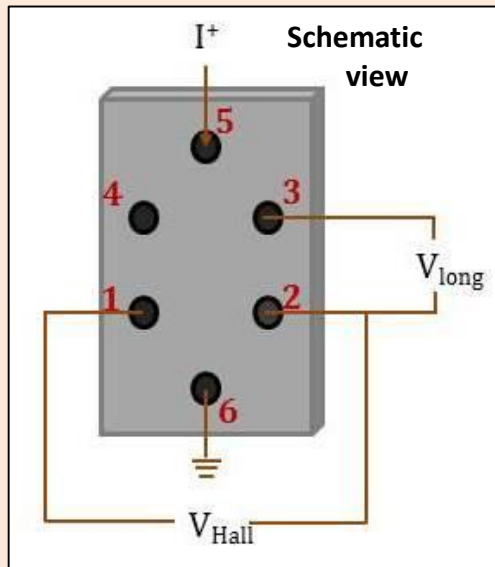
| Sample | χ_{min}^0 | χ_{min}^{irr} | $N_D (10^{20}/\text{cm}^3)$ |
|--------|-----------------|--------------------|-----------------------------|
| B | 4.44 ± 0.08 | 5.92 ± 0.06 | (6.8 ± 0.4) |
| D | 4.19 ± 0.05 | 5.76 ± 0.06 | (7.3 ± 0.4) |

Ref: M. Satoh, K. Kuriyama, Journal of Applied Physics, 67 (1990) 3890.

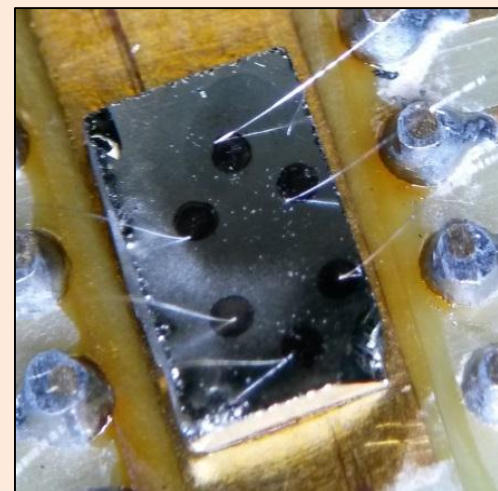
Characterizing NTD Ge sensors

Fabrication of NTD Ge

- ❖ For contact making In, Al, Au were tried and finally optimised with Au-Ge pads.
- ❖ For Hall Effect measurement six contacts pads (with Au (88 %) – Ge (12 %)) were made using standard Vander Pauw method.
- ❖ Hall Effect measurement used as tool to estimate thermal neutron dose by estimating the carrier concentration at 77K.
- ❖ The samples were rapid thermally annealed at 400°C for 2 min.
- ❖ Electrical connections were made by wedge bonding 25 μm Al wires to the contact pad.

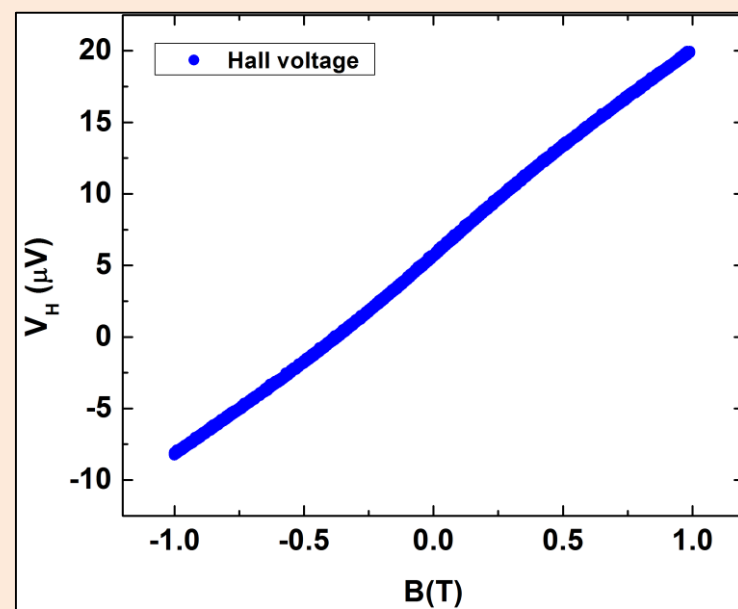
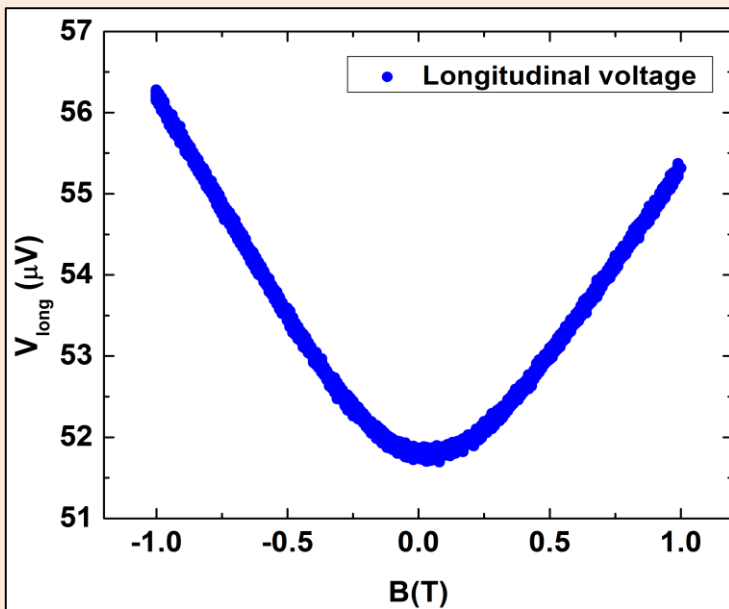


**NTD Ge with Al
wedge bonding**



Hall Effect Measurement

- ❖ The Hall voltage is measured with $100\mu\text{A}$ current in the varying magnetic field of -1 to 1 tesla.
- ❖ The Hall voltages were measured at both 77 K and at 300 K.
- ❖ Both Hall voltage and longitudinal voltage were measured simultaneously with two lockin amplifiers.



Longitudinal resistance and Hall voltage of NTD Ge sample E at 77K

Typical NTD Ge Hall Effect data

- ❖ The carrier concentration were estimated by assuming single carrier approximation using the formula:

$$V_H = \frac{B_z \cdot I_x}{n \cdot e \cdot t}$$

V_H = Hall voltage

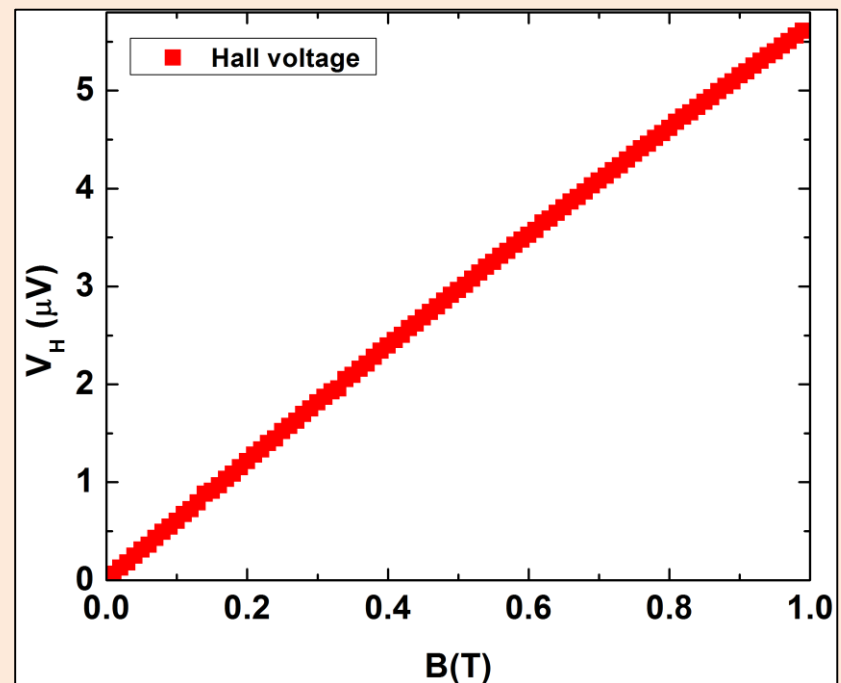
B_z = Applied Mag field

I_x = Supplied current

t = thickness

n = carrier concentration

e = charge



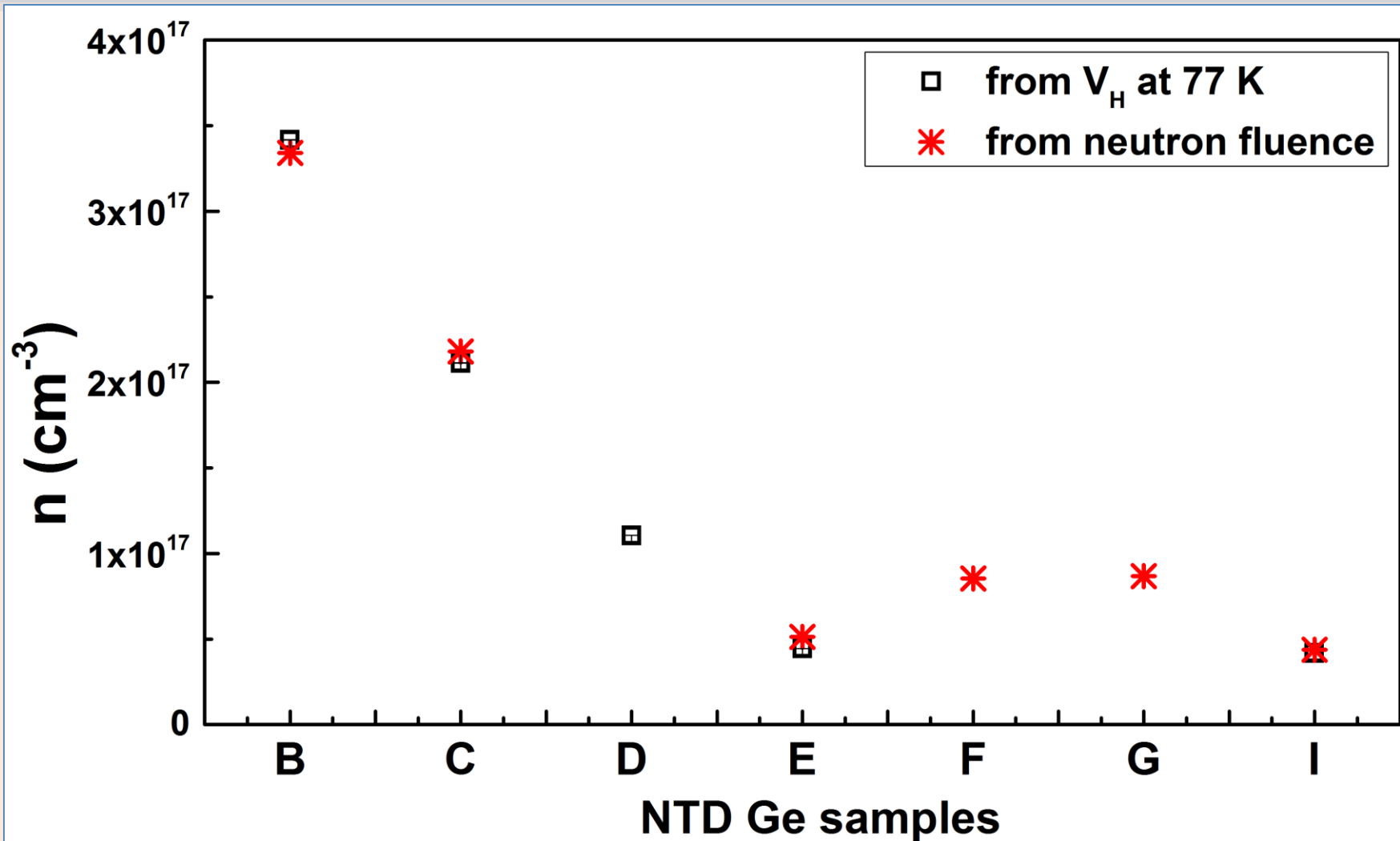
Hall Effect Result

- ❖ The contribution of magneto-resistance was taken into account during carrier concentration estimation.
- ❖ The Hall factor (Hall mobility / Hall conductivity) is close to unity* below 100K.
- ❖ At 300K the intrinsic carriers due to thermal agitation can participate in conductivity, hence the values are higher than the actual dopant concentration.

| Sample | Carrier concentration (/cm ³) error < 2% | | |
|--------|--|-----------------------|-----------------------|
| | 77K | 300K | From n-fluence |
| B | 3.42×10^{17} | 3.89×10^{17} | 3.34×10^{17} |
| C | 2.11×10^{17} | 2.60×10^{17} | 2.18×10^{17} |
| D | 1.11×10^{17} | 2.13×10^{17} | 1.11×10^{17} |
| E | 4.45×10^{16} | 7.25×10^{16} | 5.12×10^{16} |
| I | 4.17×10^{16} | 4.87×10^{16} | 4.37×10^{16} |

*F.J.Morin, Physical Review, 93 (1954) 62.

Hall Effect Results cont..



- The carrier concentration estimated using Hall Effect at 77K is compared with the carrier concentration estimated from the reactor power data.

Low temperature resistance measurement in dilution refrigerator

- ❖ A cryogen-free dilution refrigerator (CFDR-1200, Leiden make) installed at TIFR
- ❖ Minimum temperature without probe ~ 8 mK, with probe ~ 12 mK.



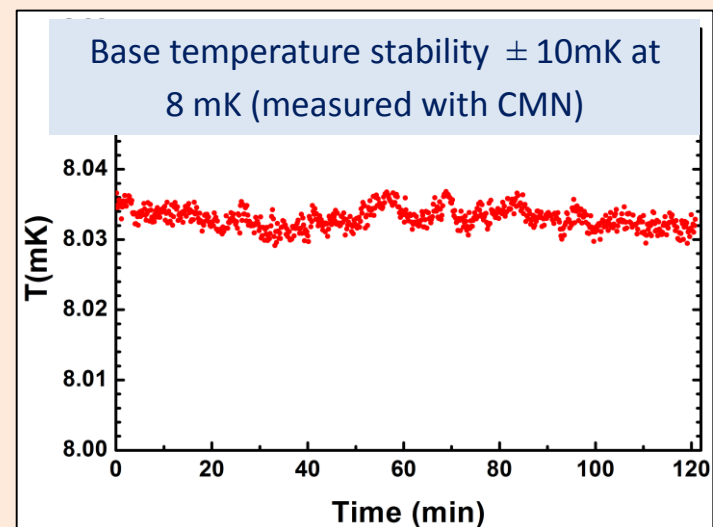
NDBD lab

Gas Handling system with the dilution unit



Probe
setup

- ❖ Cooling power 1.4 mW @120 mK with about 50 l of ^3He .
- ❖ Provision to mount electronics at 40 K stage.

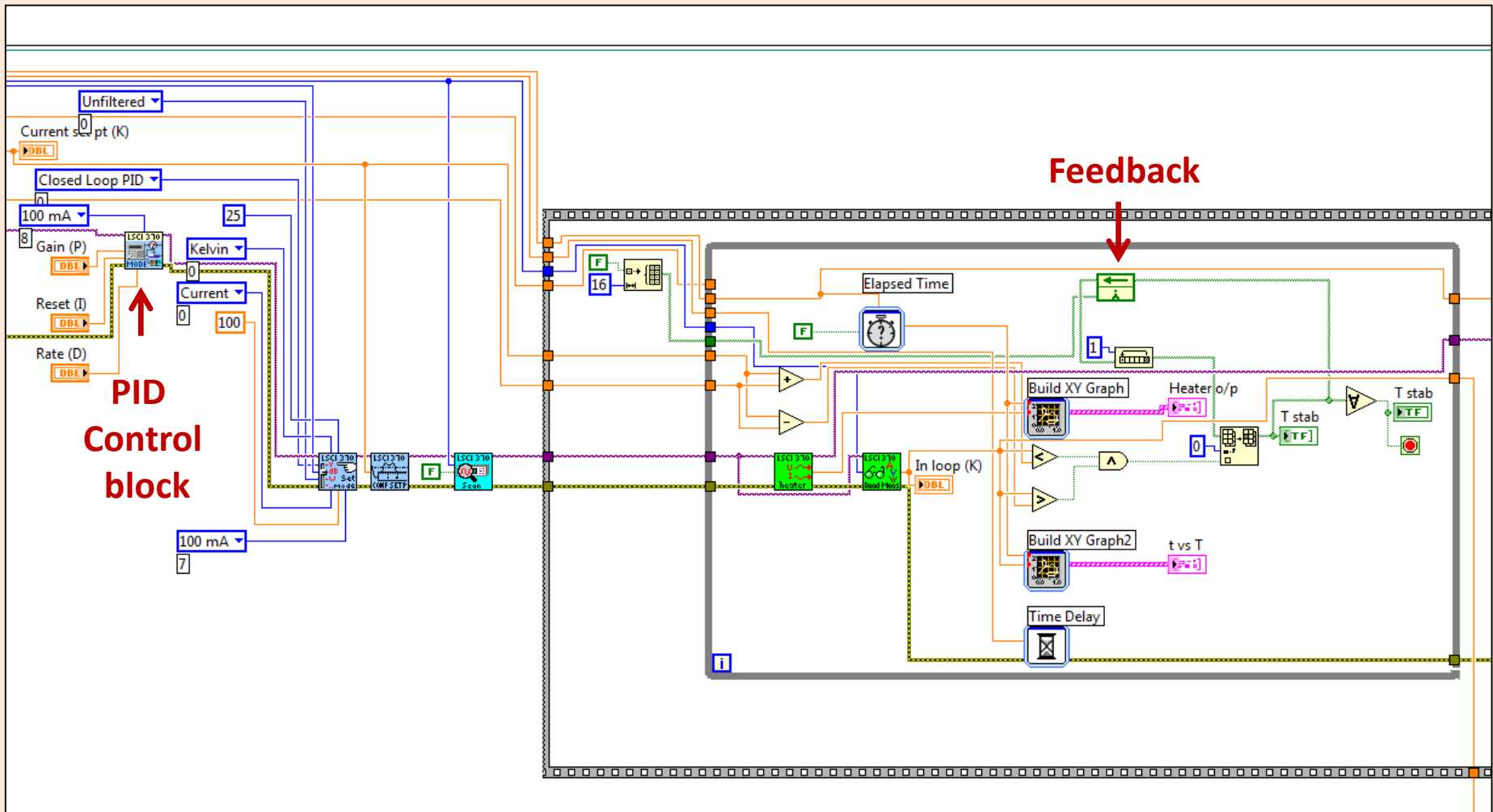


Development of DAQ system

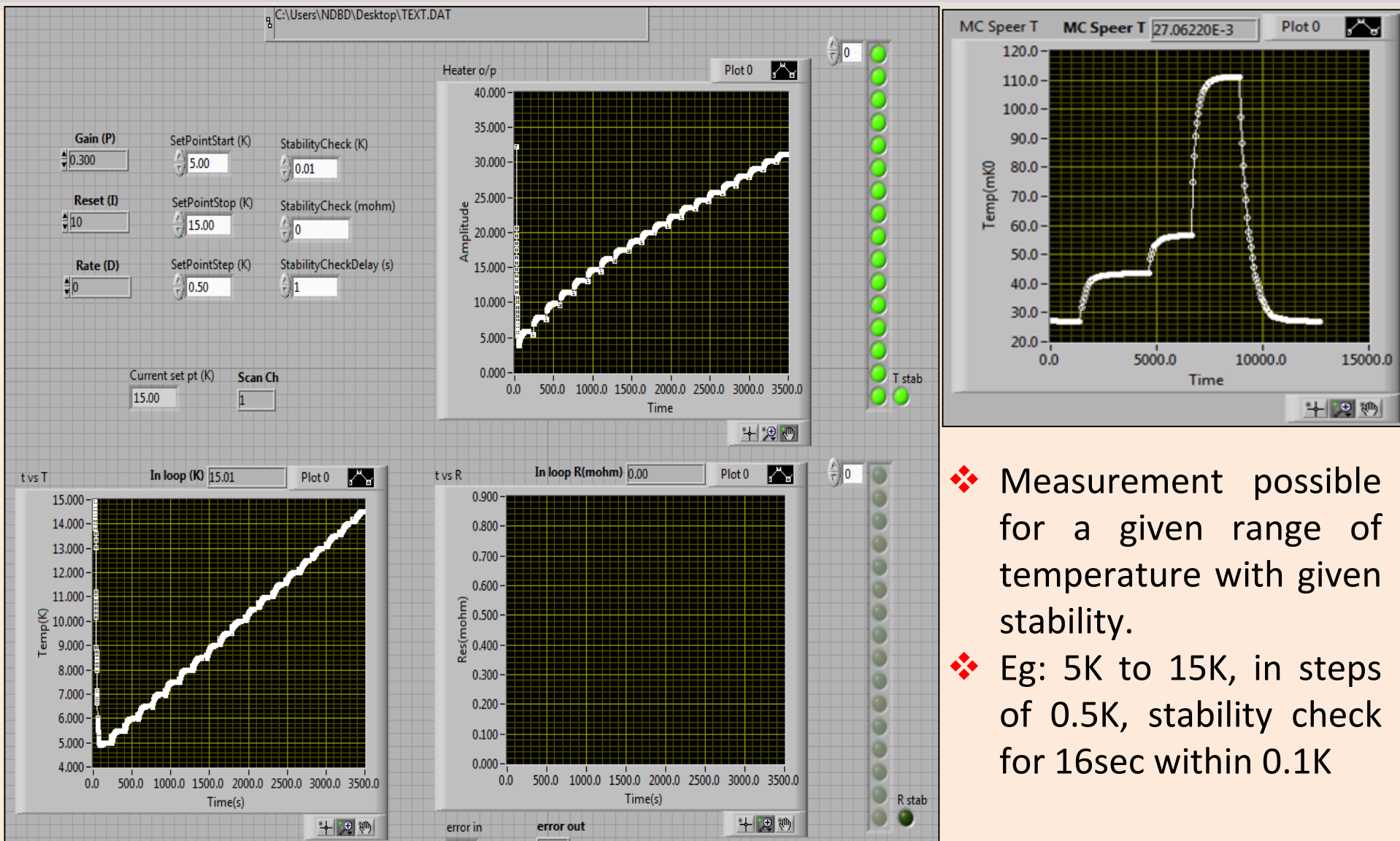


- ❖ Lakeshore, AVS 47 - the two commercial resistance bridge and NI – PXIe – 6229 were used for resistance measurement.
- ❖ Automated the 4K cryo insert and Oxford make wet dilution refrigerator with PID control.

Labview program – Block diagram



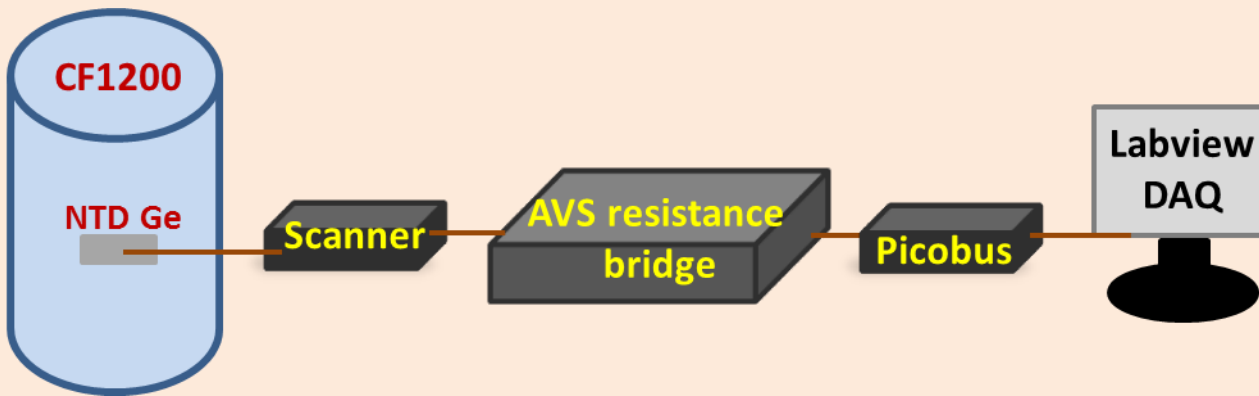
Labview program - FP



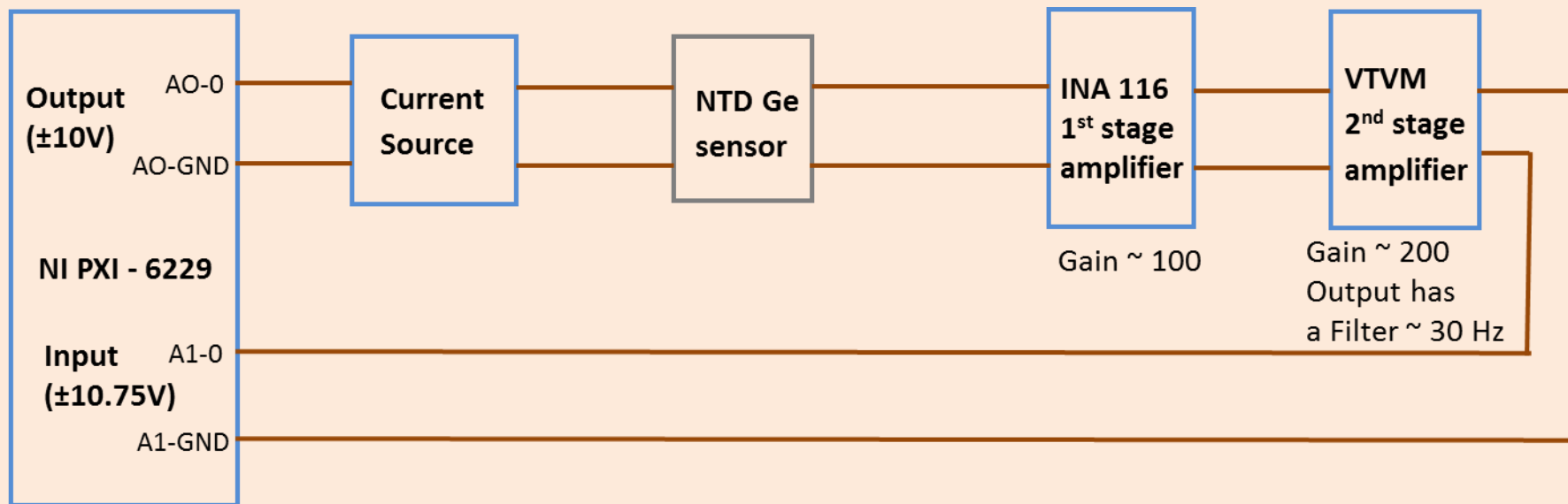
- ❖ Measurement possible for a given range of temperature with given stability.
- ❖ Eg: 5K to 15K, in steps of 0.5K, stability check for 16sec within 0.1K

Readout system

AVS Readouts



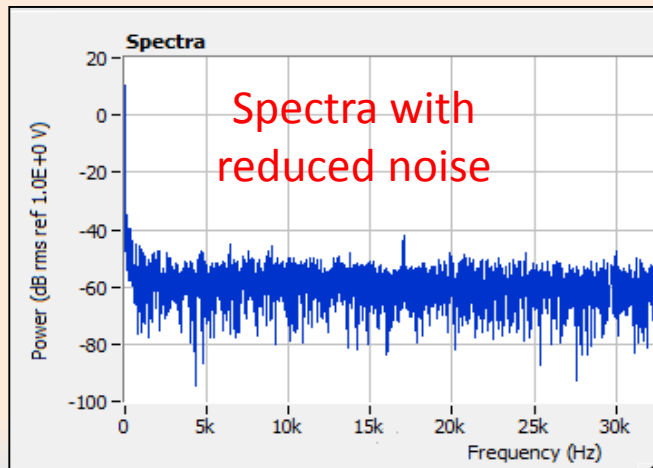
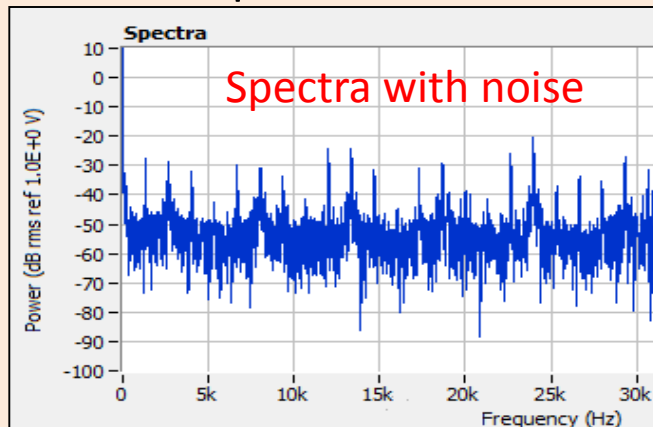
NI Readouts



Noise issues

Issues with resistance measurement:

- ❖ Thermal anchoring of the sensors
- ❖ Vibrational issues
- ❖ Grounding issues
- ❖ RF pickups
- ❖ Base temperature stabilization.

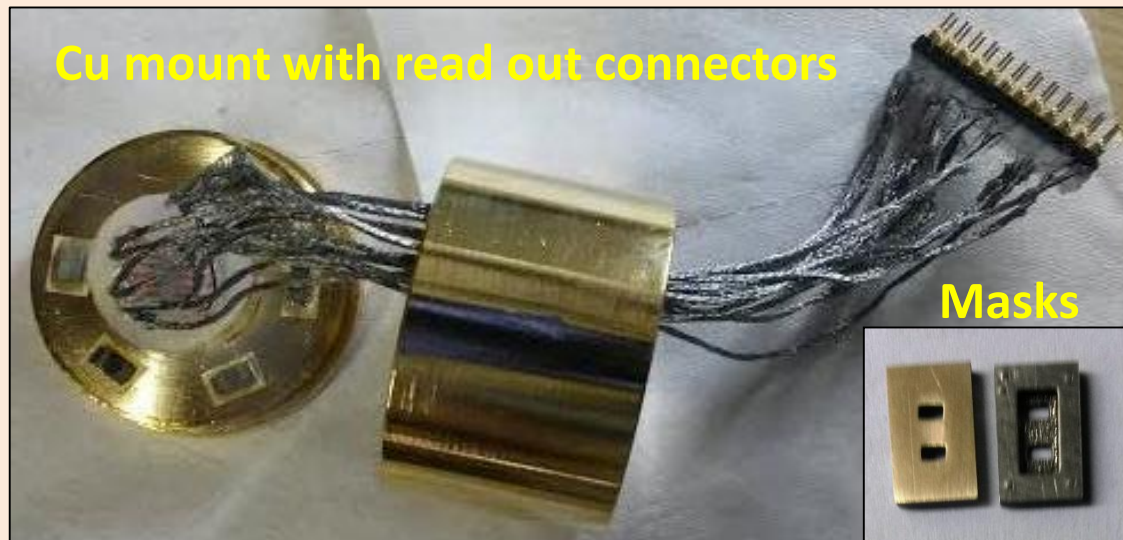
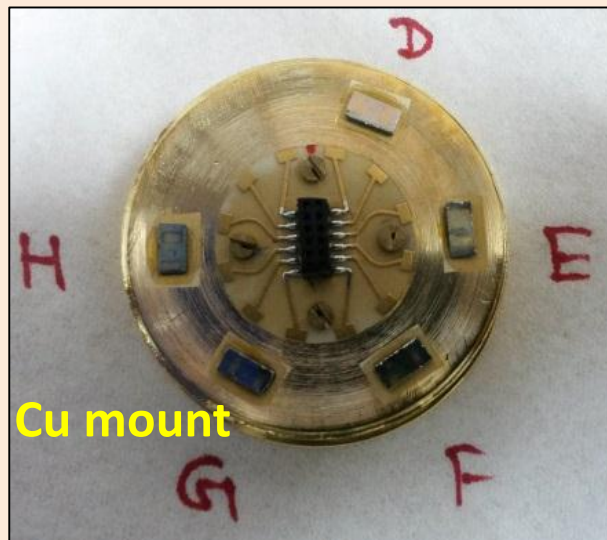
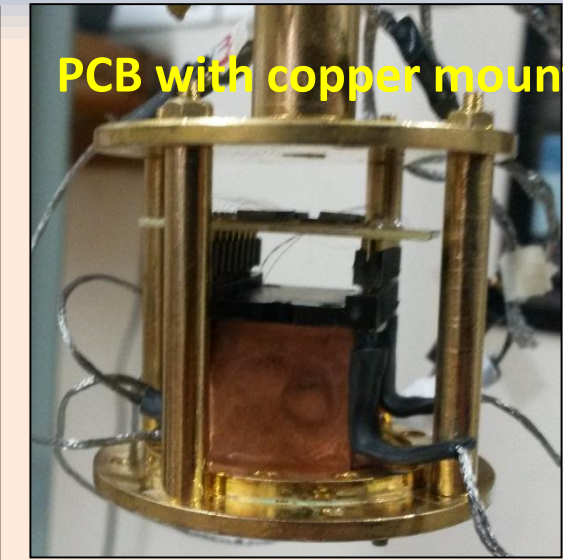
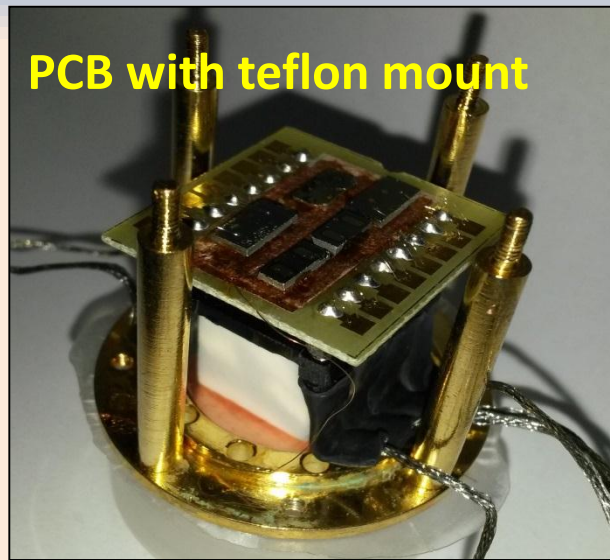
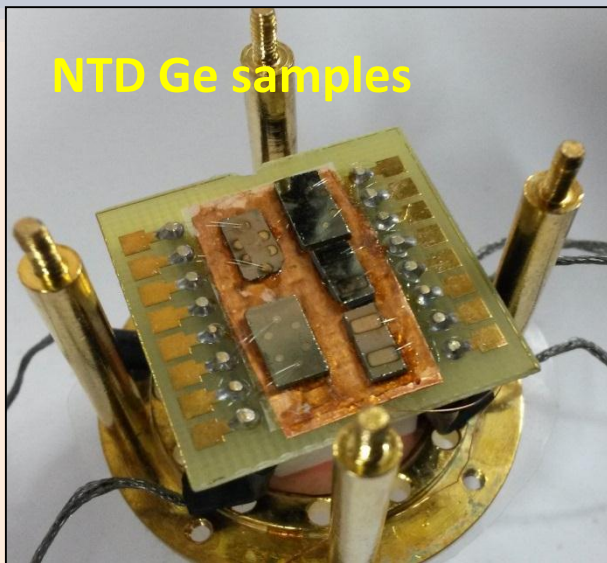


Reducing noise:

- ❖ Faraday cage
- ❖ Ground Isolator
- ❖ Vibration damper
- ❖ Suitable filter
- ❖ Shielded twisted pair cables
- ❖ EMI proof cabinet

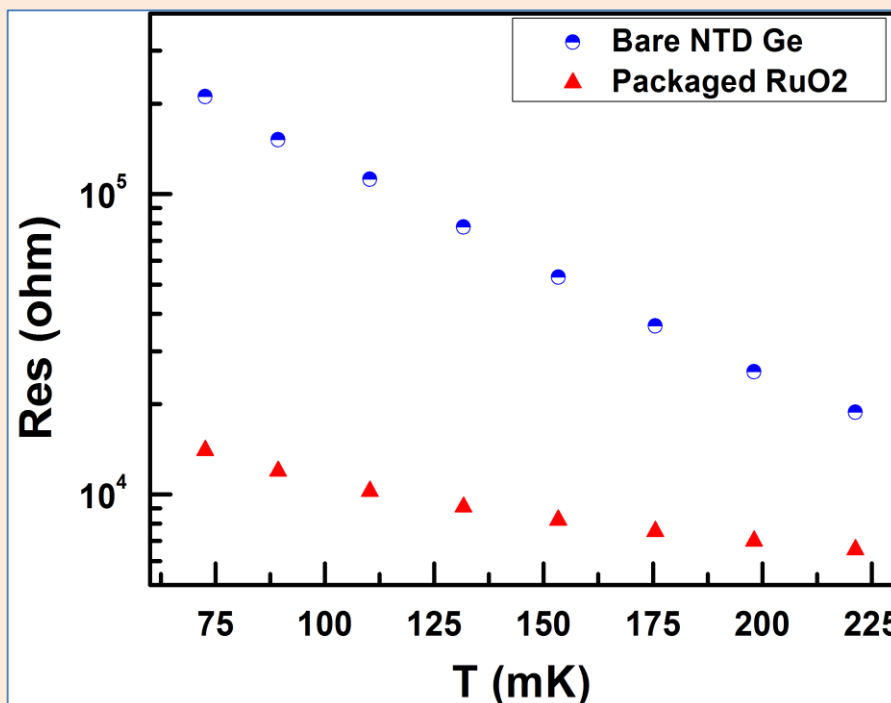


NTD Ge sample mounts



Low temperature resistance measurement (AVS)

- ❖ The samples used in Hall probe measurement were tested for low temperature resistance measurement.
- ❖ The resistance values are compared with that of commercial RuO₂ sensors.
- ❖ Clearly the NTD Ge sensor showed higher dR/dT compared to RuO₂.
- ❖ The dR/dT is about ~2.3kΩ/mK at 100mK.
- ❖ Below 75mK the NTD Ge shows saturation, which might be due to thermal link or due to the noise.

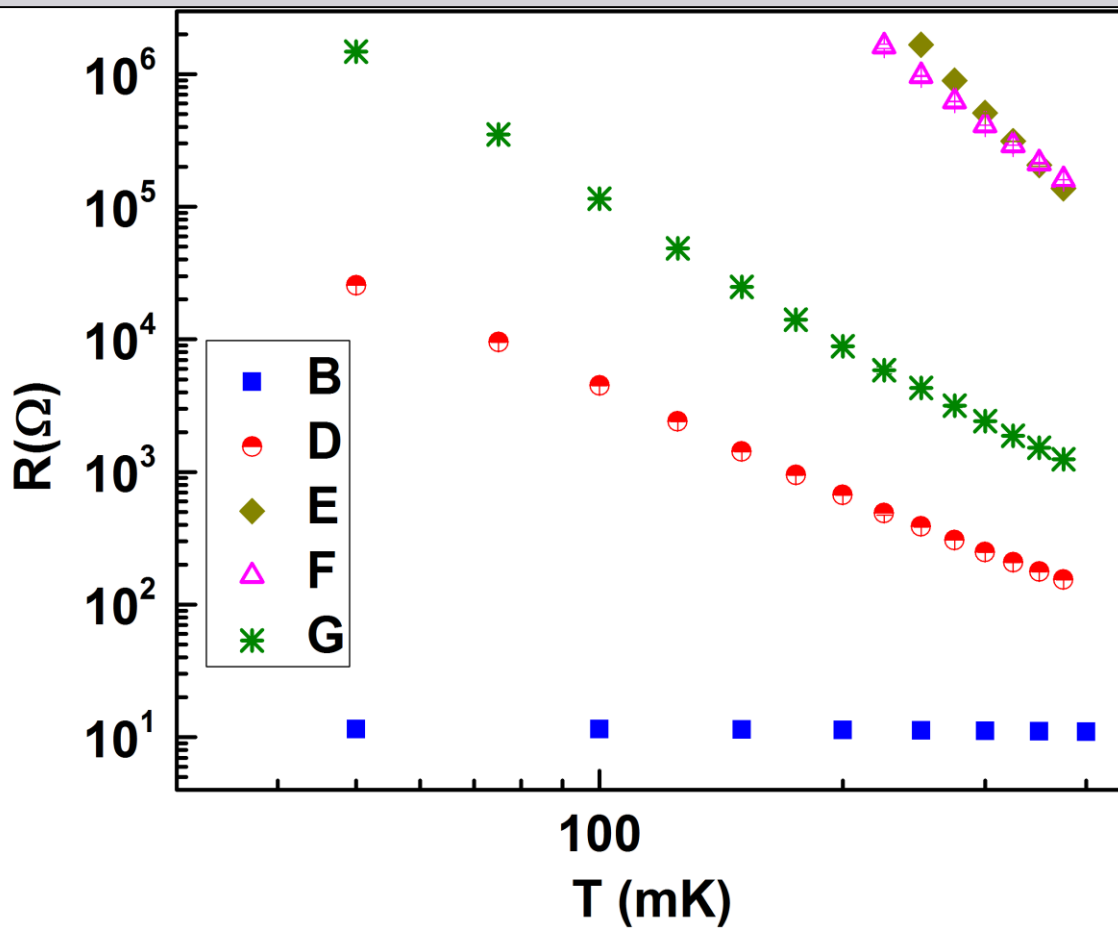


- ❖ Logarithmic sensitivity $\alpha = \left| \frac{d(\log R)}{d(\log T)} \right|$
- ❖ For a semiconductor thermistor will range between 1 to 10.

| Samples | Logarithmic sensitivity at 100mK |
|------------------|----------------------------------|
| NTD Ge | 1.7 |
| RuO ₂ | 0.7 |

- ❖ Clearly the figure of merit is higher for NTD Ge as compared to that of RuO₂.

Low temperature resistance measurement cont..



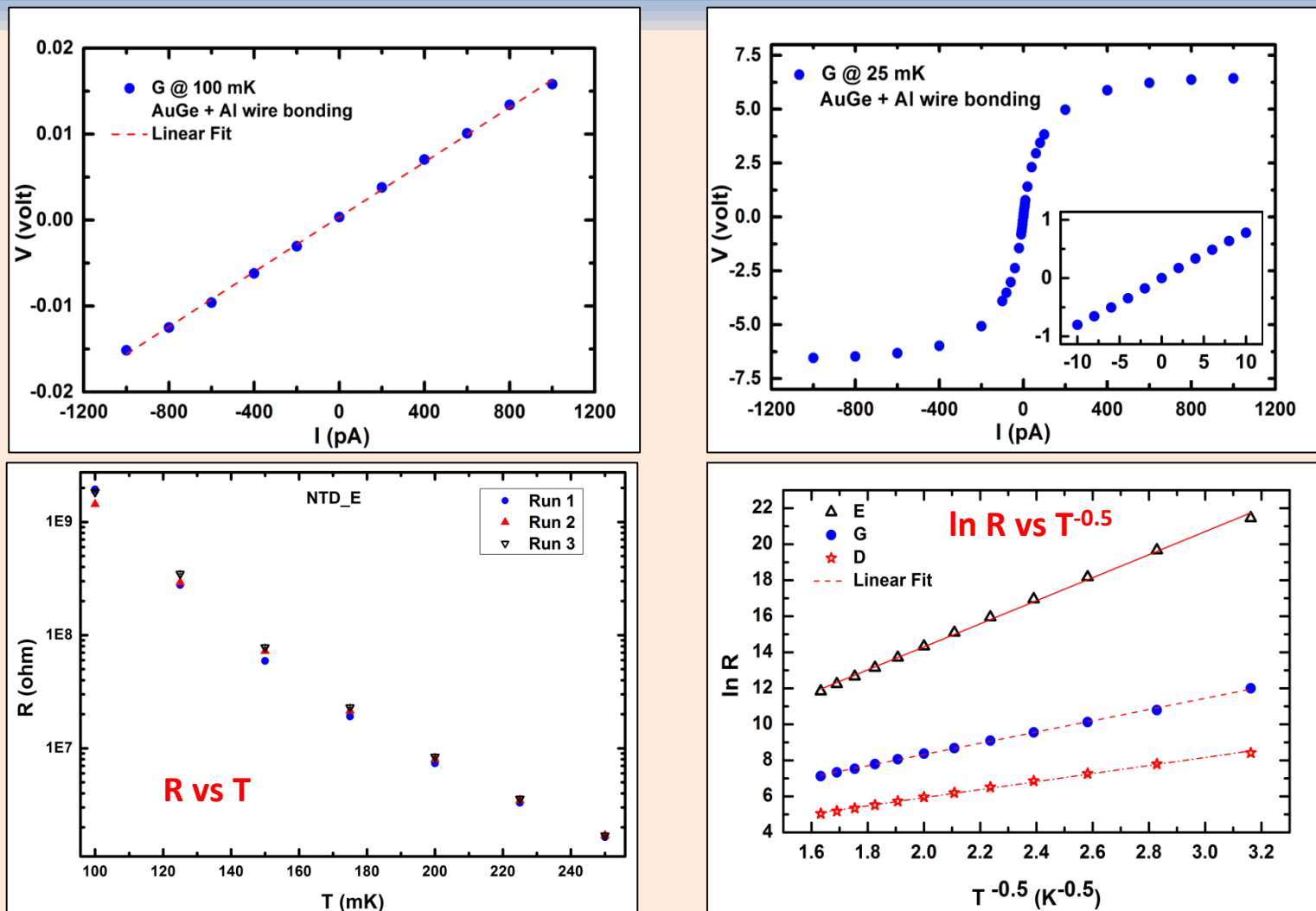
$N_A - N_D$ from Hall Effect:

| NTD Ge | Carriers/cm ³ |
|--------|--------------------------|
| B | 3.42 x 10 ¹⁷ |
| D | 1.11 x 10 ¹⁷ |
| E | 4.45 x 10 ¹⁶ |
| *F | 8.55 x 10 ¹⁶ |
| *G | 8.68 x 10 ¹⁶ |
| H | 4.17 x 10 ¹⁶ |

*Estimated from reactor power data

- ❖ Resistance measured using AVS resistance bridge as a function of temperature for various neutron fluence.
- ❖ Sample NTD H has very large resistance even at 400mK, hence could not measure.

VI measurement using NI-PXle



❖ The logarithmic resistance of NTD Ge goes linear with $T^{-0.5}$.

Extracted parameters of NTD Ge

For NTD Ge sensor $R = R_0 \exp\left[\frac{T_0}{T}\right]^\alpha$

(E. Pasca *et al.*, Proc. 8th Int. Conf. Adv. Tech. Part. Phys. **2** (2004) 93)

R_0 depends on intrinsic properties of Ge, T_0 depends on the doping level and constant $\alpha \sim 0.5$ (A.L. Woodcraft *et al.*, J. Low Temp. Phys. **134** (2004) 925)

| Sample | Carrier concentration (/cm ²) | T ₀ (K) | R ₀ (Ω) |
|--------|---|--------------------|--------------------|
| D | 4.57 x 10 ¹⁸ | 5.02(0.02) | 4.2(0.1) |
| G | 3.57 x 10 ¹⁸ | 9.78(0.06) | 7.9(0.2) |
| E | 2.11 x 10 ¹⁸ | 41.1(0.3) | 4.4(0.2) |

Variation in R₀ can be due to residual stress, unannealed radiation damage etc. (also reported by N. Wang *et al.*, Phys. Rev. B **41** (1990) 3761).

A. Garai, S. Mathimalar *et al.*, JLTP proceedings (In press) .

Summary

- ❖ NTD Ge sensor is chosen for the upcoming TIN.TIN (NDBD experiment at INO).
- ❖ Ge wafers are doped by neutron transmutation doping technique.
- ❖ Both PALS and Channeling confirmed that annealing the irradiated samples at 600°C for 2hrs in a sealed quartz tube can reduce the defects formed due to fast neutrons.
- ❖ Hall probe measurement at 77K is used as a tool to verify the neutron fluence.
- ❖ NTD Ge ($\phi_{th} = 4.6 \times 10^{18}/\text{cm}^2$) has higher dR/dT compared to that of the commercial RuO₂.
- ❖ For our semiconductor grade natural Ge, $\phi_{th} > 10^{19}/\text{cm}^2$ ($N_A - N_D: 3.42 \times 10^{17}$) shows metallic behaviour.
- ❖ Preferable neutron fluence for natural Ge samples:
 $2 \times 10^{18}/\text{cm}^2 < \phi_{th} < 5 \times 10^{18}/\text{cm}^2$.
(corresponding carrier concentration: **$4 \times 10^{16}/\text{cm}^3 < N_A - N_D < 11 \times 10^{16}/\text{cm}^3$**).

List of Publications

Publications in Refereed Journal:

- (i) Study of radioactive impurities in neutron transmutation doped Ge, **S. Mathimalar**, et al., Nucl. Instr. and Meth. A, 774 (2015) 68.
- (ii) Characterization of neutron transmutation doped (NTD) Ge for low temperature sensor development, **S. Mathimalar**, et al., Nucl. Instr. and Meth. B, 345 (2015) 33.

Publications in Proceedings:

- (i) Development of NTD Ge sensors for low temperature thermometry, **S. Mathimalar**, et al., International Workshop on Low Temperature Electronics 2014, Proceedings of IEEE Explore, doi:10.1109/WOLTE.2014.6881014.

Other Publications:

- (i) Specific Heat of Teflon, Torlon - 4203 and Torlon - 4301 in the range of 30 -400 mK, V. Singh, A. Garai, **S. Mathimalar**, et al., Cryogenics, 67 (2015) 15.
- (ii) Heat capacity setup for superconducting bolometer absorbers below 400mK, V. Singh, **S. Mathimalar**, et al., Journal of Low Temperature Physics, 175 (2014) 604.
- (iii) Cryogen Free Dilution Refrigerator for bolometric search of neutrinoless double decay ($0\nu\beta\beta$) in ^{124}Sn , V. Singh, **Mathimalar. S**, et al., Pramana - Journal of Physics, 81 (2013) 719.
- (iv) Characterization and modeling of a low background HPGe detector, N. Dokania, V. Singh, **S. Mathimalar**, et al., Nucl. Instrum. Meth. A, 745 (2014) 119.
- (v) Study of neutron-induced background and its effect on the search of 0 decay in ^{124}Sn , N. Dokania, V. Singh, **S. Mathimalar**, et al., Journal of Instrumentation, doi:10.1088/1748-0221/9/11/P11002.

Collaborators

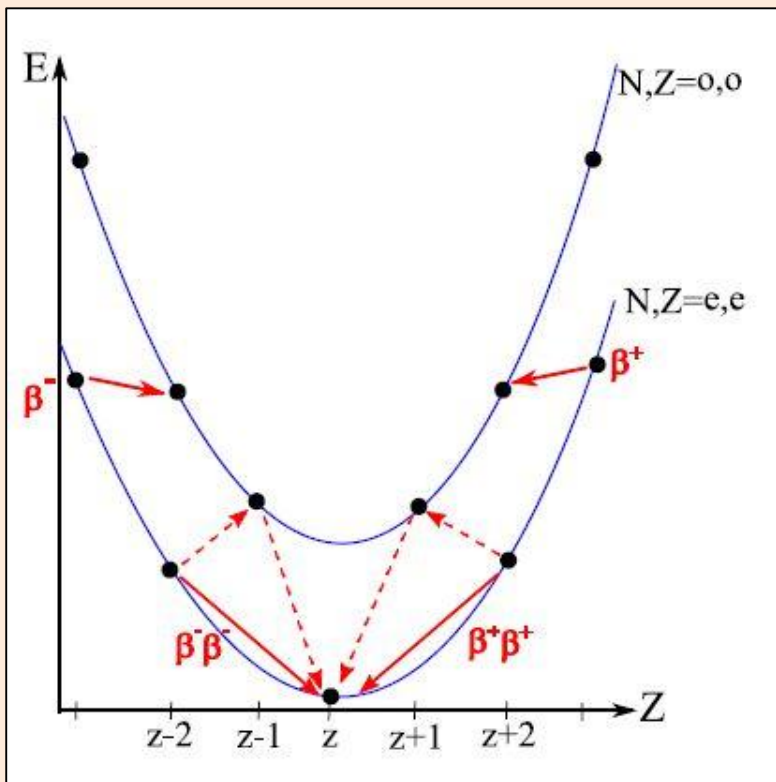
Dr. V Singh
Dr. Neha Dokania
Mr. Abhijit Garai
Prof. V. Nanal
Prof. R.G. Pillay
Dr. Sanjoy Pal
Prof. S. Ramakrishnan
Dr. A. Shrivastava
Dr. Priya Maheswari
Dr. P.K. Pujari
Mr. Sunil Ojha
Dr. D. Kanjilal
Mr. K.C. Jagadeesan
Dr. S.V. Thakare

Acknowledgement

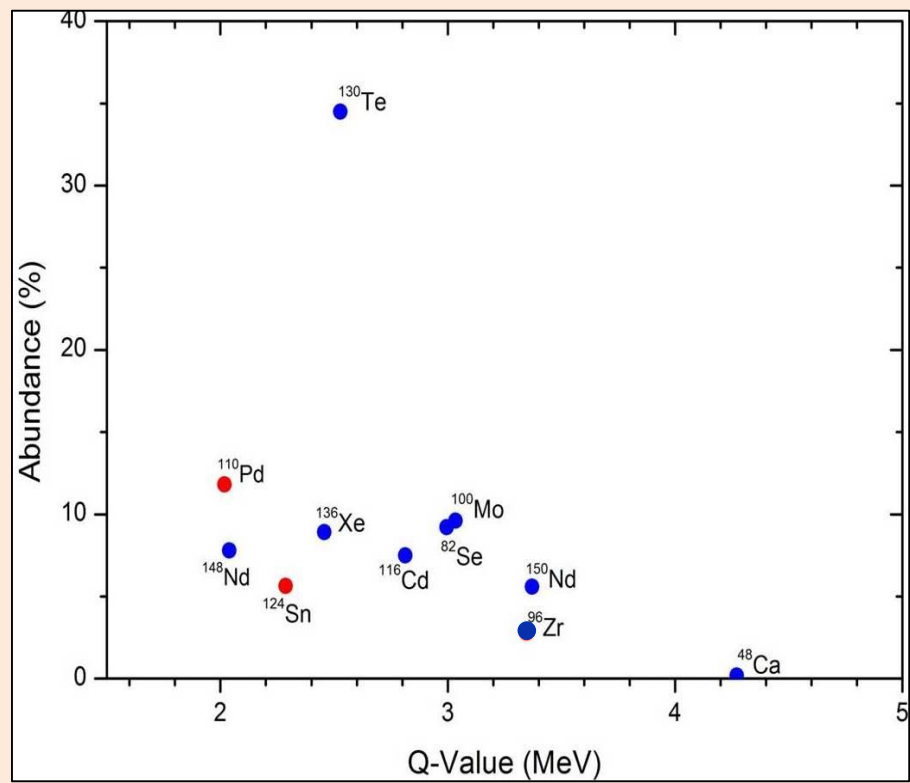
Dr. G. Ravikumar
Prof. V.M. Datar
Prof. Mandar Deshmukh
Prof. Shriganesh S. Prabhu
Ms. Sadhana Mishra
Mr. J.N. Karande
Mr. Mahesh Pose
Mr. Chandan Ghosh
Mr. Kiran Divekar
Mr. Mallikarjunachary
Ms. Sudipta Dubey
Mr. John Mathew
Mr. Abhishek Singh
Mr. Harshad S Surdi
Mr. Rudheer D Bapat
Ms. Bagyshri A Chalke

Thank you

Nuclei decay via DBD



Mass parabola of even A



Nuclei undergoing DBD ($Q > 2\text{ MeV}$)

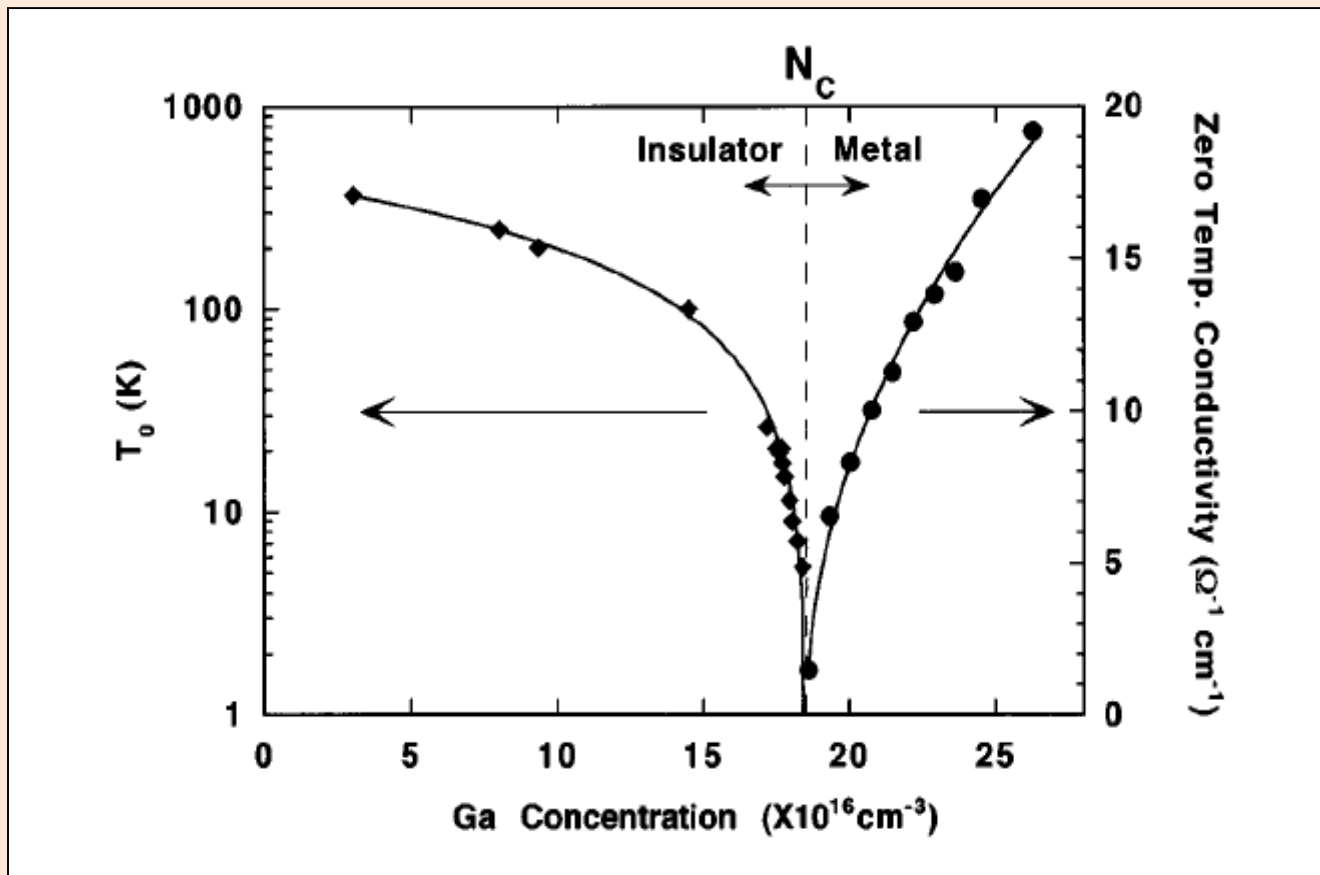
❖ ^{124}Sn is one of the nuclei which undergoes $\beta\beta$ decay

T_{1/2} limits of 0νββ

Table : $\beta\beta$ candidates with Q values greater than 2 MeV. The SM process of 2νββ decay has been observed in most of the candidates while only limits exists for 0νββ process.

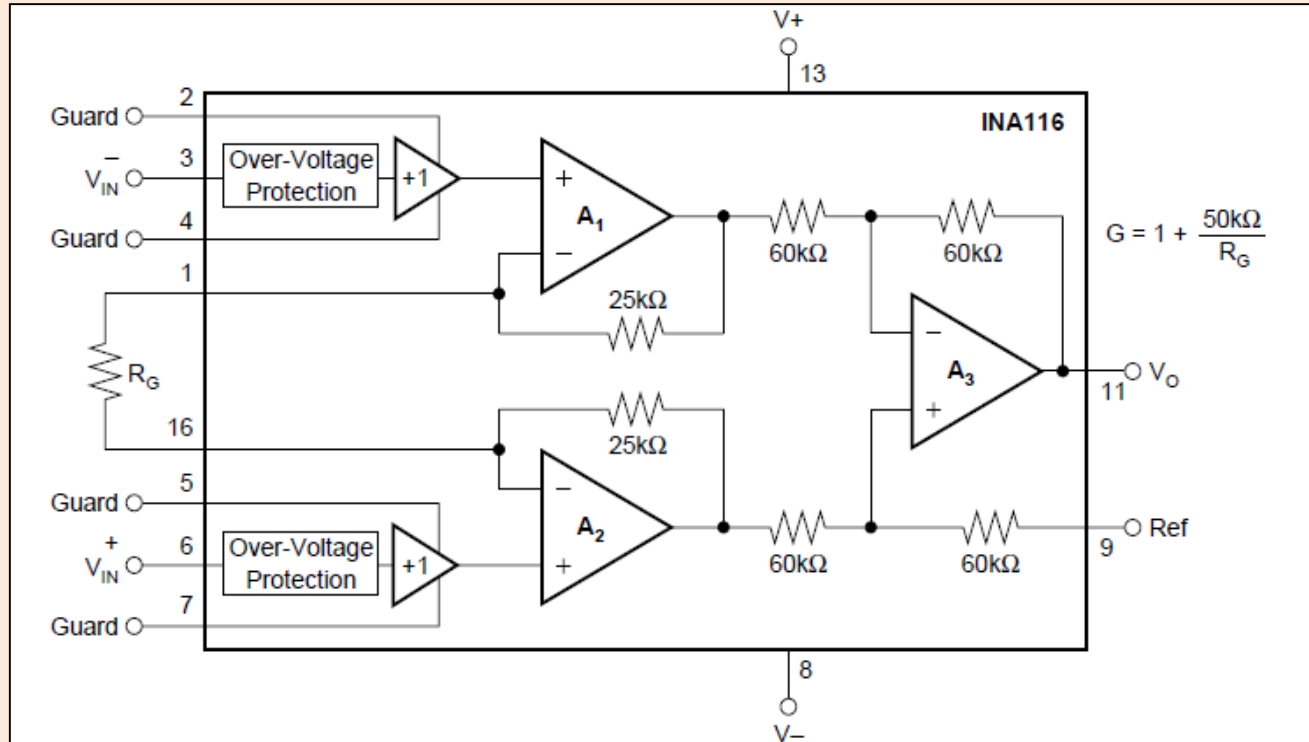
| Isotope | Q_{value} (keV) | Nat. Abun. (%) | $T_{1/2}^{2\nu}$ (yrs) | $T_{1/2}^{0\nu-exp}$ (yrs) |
|-------------------|----------------------|-------------------|------------------------------------|-------------------------------|
| ⁴⁸ Ca | 4362 ± 0.84 | 0.187 | $4.4_{-0.5}^{+0.6} \cdot 10^{19}$ | $> 1.4 \cdot 10^{22}$ |
| ⁷⁶ Ge | 2039.006 ± 0.050 | 7.73 | $1.6_{-0.1}^{+0.13} \cdot 10^{21}$ | $> 2.1 \cdot 10^{25}$ |
| ⁸² Se | 2997.9 ± 0.3 | 8.73 | $0.92 \pm 0.07 \cdot 10^{20}$ | $> 3.6 \cdot 10^{23}$ |
| ⁹⁶ Zr | 3347.7 ± 2.2 | 2.80 | $2.3 \pm 0.2 \cdot 10^{19}$ | $> 9.2 \cdot 10^{21}$ |
| ¹⁰⁰ Mo | 3034.40 ± 0.17 | 9.82 | $7.1 \pm 0.4 \cdot 10^{18}$ | $> 1.1 \cdot 10^{24}$ |
| ¹¹⁰ Pd | 2017.85 ± 0.64 | 11.72 | $> 6.0 \cdot 10^{16}$ | $> 6.0 \cdot 10^{16}$ |
| ¹¹⁶ Cd | 2813.50 ± 0.13 | 7.49 | $2.85 \pm 0.15 \cdot 10^{19}$ | $> 1.7 \cdot 10^{23}$ |
| ¹²⁴ Sn | 2292.64 ± 0.39 | 5.79 | $> 1.0 \cdot 10^{17}$ | $> 2.0 \cdot 10^{19}$ |
| ¹³⁰ Te | 2527.518 ± 0.013 | 34.08 | $6.9 \pm 1.3 \cdot 10^{20}$ | $> 2.8 \cdot 10^{24}$ |
| ¹³⁶ Xe | 2457.83 ± 0.37 | 8.86 | $2.20 \pm 0.06 \cdot 10^{21}$ | $> 1.9 \cdot 10^{25}$ |
| ¹⁵⁰ Nd | 3371.38 ± 0.20 | 5.64 | $8.2 \pm 0.9 \cdot 10^{18}$ | $> 1.8 \cdot 10^{22}$ |

Critical concentration (MIT)



Readout system

INA116 – 1st stage amplifier



Voltage noise

$f = 1\text{kHz} \sim 28 \text{ nV}/\sqrt{\text{Hz}}$
 $f_B = 0.1\text{Hz}$ to $10\text{Hz} \sim 2\mu\text{V p-p}$

Current noise

$f = 1\text{kHz} \sim 0.1 \text{ fA}/\sqrt{\text{Hz}}$

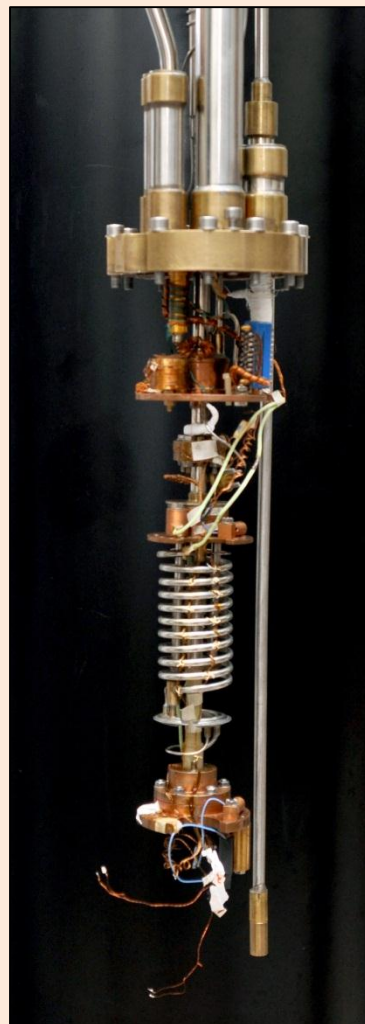
- ❖ **Current source** is a Voltage to Current converter with an output adjustment range of $\pm 1000 \text{ pA}$.
- ❖ The voltage to the unit is supplied by an analog output channel of NI-PXI 6229 (16 bit DAC)

Refurbished wet oxford dilution Refrigerator

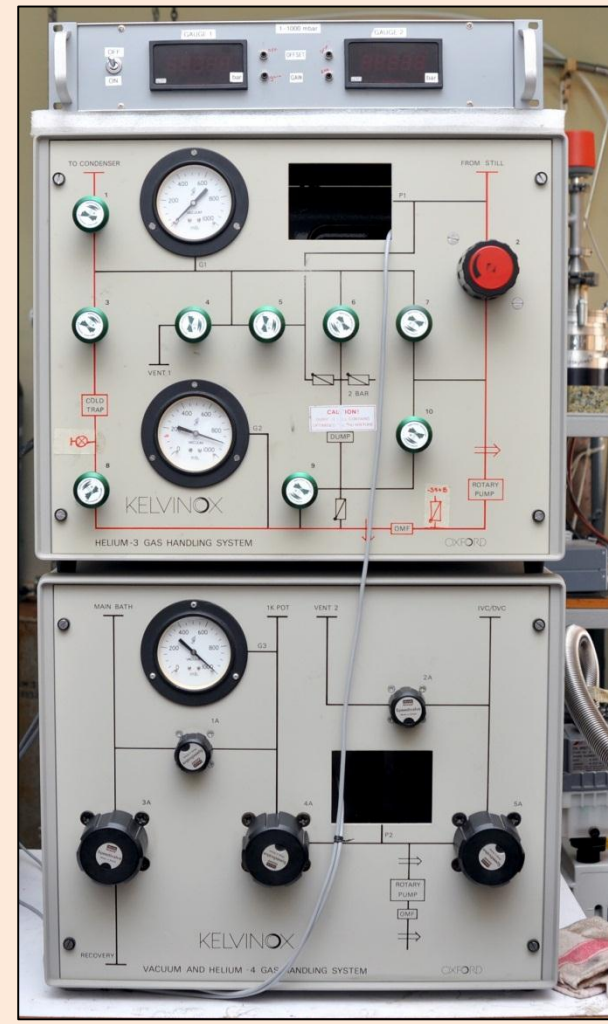
Dilution Refrigerator



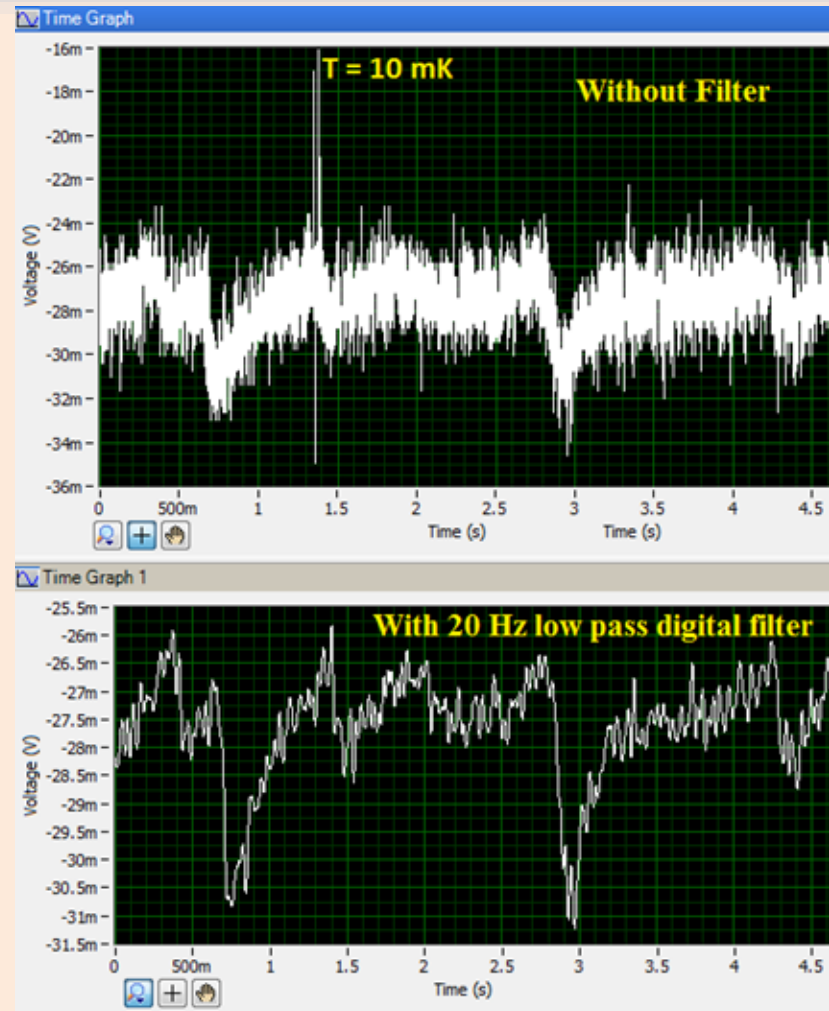
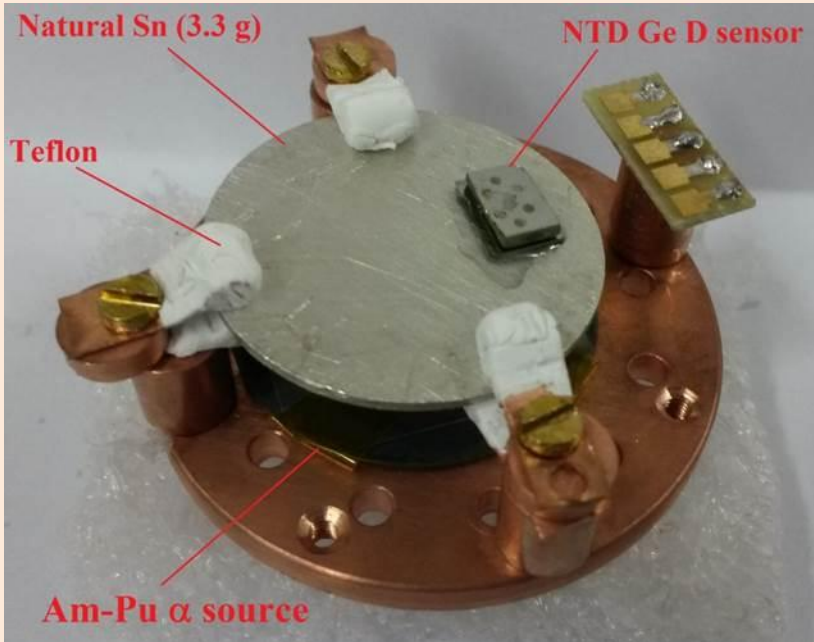
Insert



Gas systems



Prototype Bolometer

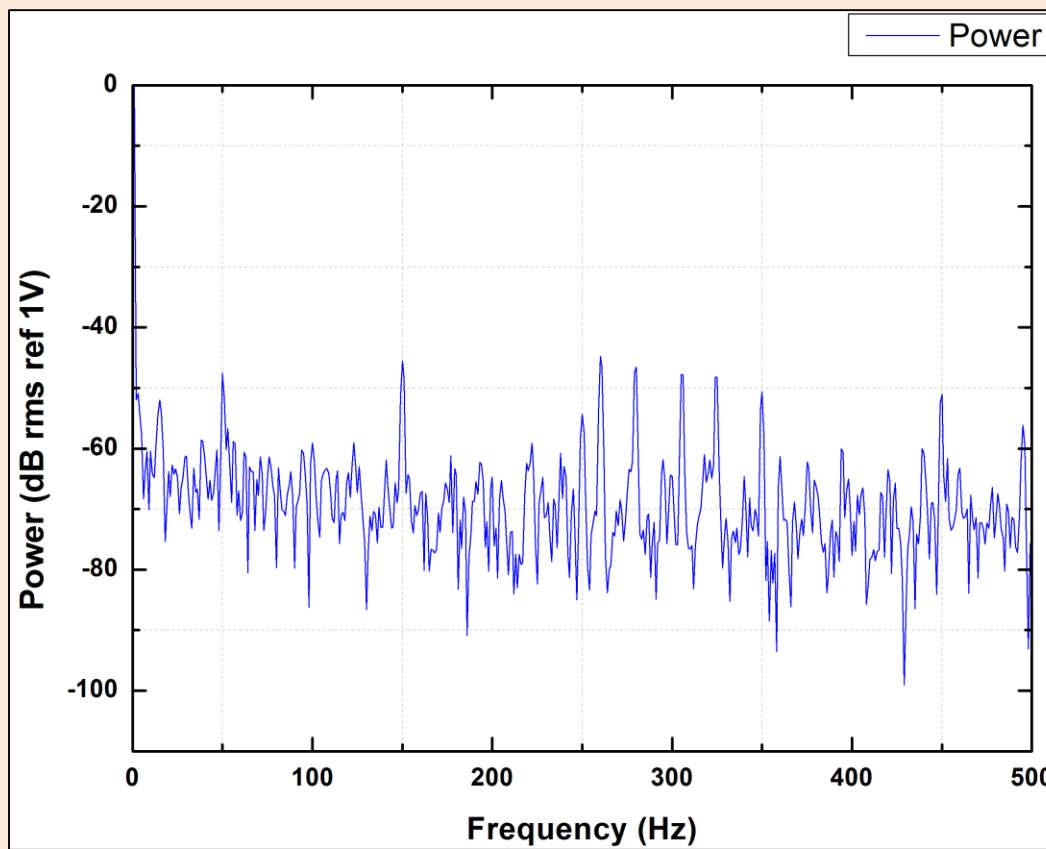


4K Cryoinsert for resistivity measurements between 4 to 300K

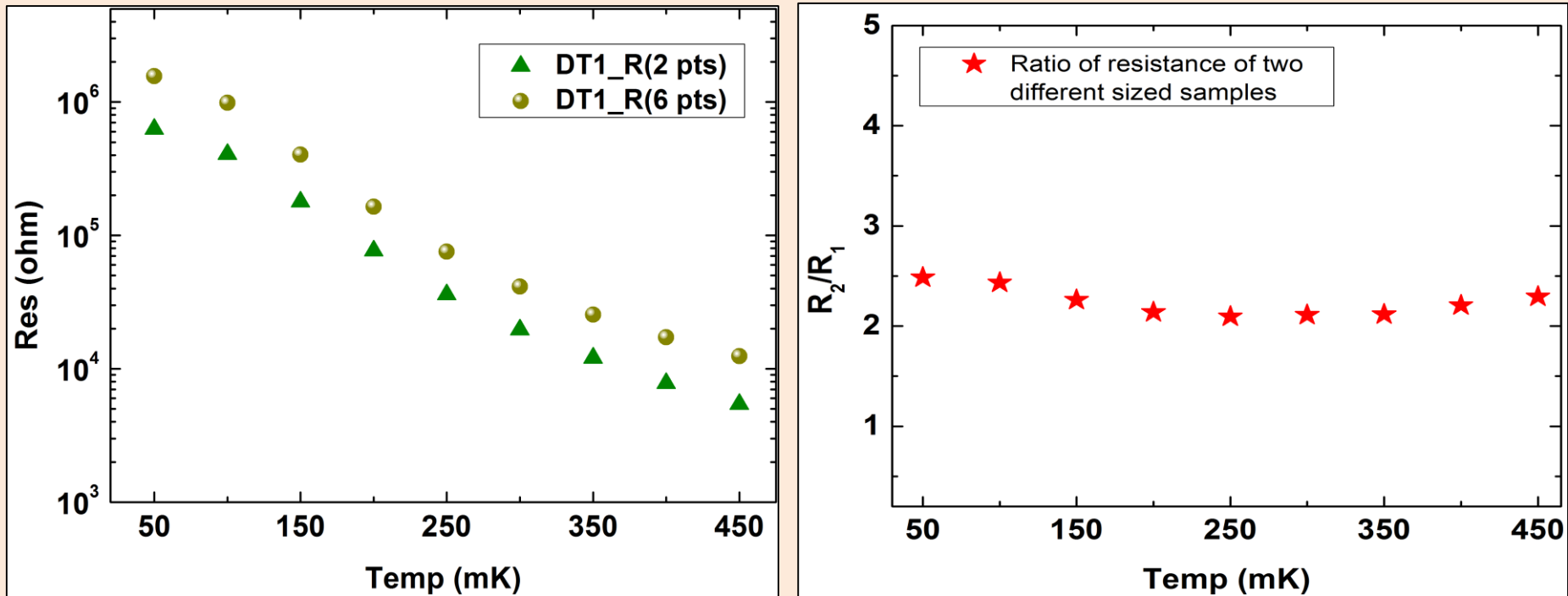


- ❖ In order to measure the resistivity of the samples from room temperature down to 4K, an insert has been designed and fabricated with SS material.
- ❖ This insert was also used to check the behavior of electrical contacts after thermal cyclings.

Noise level at lower frequency



Example for Homogenous doping (NTD Ge D)



Future scope

- ❖ Sensor in the bolometer basically measures the phonon signal from the absorber.
- ❖ Signal depends on specific heat of the absorber and weak heat link, which provides detector time constant (τ_d).
- ❖ At very low temperature the phonon-electron decoupling in sensor can happen, which provides an additional intrinsic time constant (τ_i).
- ❖ Knowledge of τ_i is essential in terms of detector performance, as it can provide additional noise due to thermodynamical fluctuations between electron and phonon bath.
- ❖ The Physics issues – **intrinsic time constant (τ_i) should be α (logarithmic sensitivity) times less than detector time constant (τ_d)**, τ_i dependence on neutron dose can be measured and the n-dose can be optimized. This also gives an idea of Hot electron model.